Welding in the World
https://doi.org/10.1007/s40194-026-02335-z

RESEARCH PAPER

Selected applications of artificial intelligence and machine learning in metal additive manufacturing

David W. Rosen[1,2] · **Xiaofang Liu**[1]

Received: 7 October 2025 / Accepted: 6 January 2026

Abstract
Additive manufacturing (AM) represents a category of manufacturing processes that fabricates parts in a layer-by-layer manner. As such, AM provides unique advantages over conventional manufacturing processes such as the ability to fabricate highly complex geometries, to minimize material waste, and to enable mass customization, while having some limitations, such as high costs and complexities. Advances in artificial intelligence (AI) and machine learning (ML) enable these limitations to be addressed due to the data-rich environment in modern commercial AM machines with multiple sensors. This paper surveys papers that apply AI/ML techniques to the topics of defect detection, AM process surrogate models and their application, generative design, and design for manufacturing in metal AM processes. The approach taken is to introduce these topics, provide a coarse survey, and then discuss specific applications in some depth, rather than to provide a fine-grained, comprehensive survey.

Keywords Artificial intelligence · Machine learning · Additive manufacturing · Defect detection · Surrogate models · Generative design · Design for manufacturing

1 Introduction

Additive manufacturing (AM) (informally called 3D printing) is used in a variety of high value applications in the aerospace, biomedical, and energy industries, among others. Due to the fabrication approach of adding and processing material in a layer-by-layer manner, AM offers unique advantages over conventional manufacturing processes such as the ability to fabricate highly complex geometries, minimize material waste, and enable mass customization [1]. However, AM processes broadly still have limitations including long build times and high costs. Metal AM processes, which are of primary interest in this paper, involve complex thermomechanical interactions that are sensitive to process settings, feedstock and build environment variability, part shape details, and many other factors. These factors contribute to variability in microstructures, mechanical properties, surface finish, and dimensional accuracy that can lead to inhomogeneous and anisotropic properties and to unpredictability in terms of performance requirements.

Artificial Intelligence (AI) and Machine Learning (ML) have advanced rapidly in recent years to become a promising tool set for addressing these limitations. Commercial AM machines often have a variety of sensors that capture process data, such as melt pool images and temperature distributions. These data, combined with emerging material characterization datasets, can enable AI/ML model development across the product development workflow, for example, for design optimization, process planning, in-situ monitoring, defect detection, and post-process inspection. This integration has the potential to enhance both the efficiency and reliability of AM, thereby accelerating its adoption in production manufacturing by enabling data-driven quality assurance and part and process qualification.

More specifically, AI/ML methods can often extract actionable insights from the high-dimensional datasets of metal AM that require methods beyond traditional

Recommended for publication by Commission I - Additive Manufacturing, Surfacing, and Thermal Cutting

✉ David W. Rosen
rosendw@a-star.edu.sg

[1] George W, Woodruff School of Mechanical Engineering, Georgia Institute of Technology, Atlanta, GA 30332, USA

[2] Institute of High Performance Computing, Agency for Science, Technology, and Research (A*STAR), 1 Fusionopolis Way, #16-16 Connexis, Singapore 138632, Republic of Singapore

Published online: 31 January 2026

physics-based modeling. AI/ML algorithms can identify nonlinear correlations, detect subtle anomalies, and provide predictive insights that would be difficult using conventional modeling approaches. In addition to process parameter tuning, AI/ML also supports higher-level objectives such as reducing support structures, minimizing residual stresses, and tailoring microstructures. By embedding intelligence into AM workflows, companies can pursue production manufacturing using AM, by reducing the need for costly post-build inspection and increasing confidence in as-built part quality.

In this paper, applications of AI/ML in metal AM defect detection and on-line monitoring, surrogate models of AM processes, generative design, and design for manufacturing are summarized. Capabilities and limitations of the AI/ML methods will be highlighted, offering insights into future research directions. Many technical articles and review papers have been written about AI/ML in manufacturing and AM, in particular [2–7]. Rather than take a similar approach, this paper covers examples in each area mentioned in some depth to illustrate how AI/ML operates and why it succeeds, rather than breadth of coverage. We focused on two topics of considerable interest, defect detection and surrogate models, one topic of increasing interest, generative design, and one topic that is just starting to receive attention, design for manufacturing.

The review methodology to identify relevant literature will be described. We conducted the search primarily using Google Scholar, covering publications from 2015 to 2025. Search queries combined terms related to metal AM processes, AI/ML approaches, defect detection, surrogate modeling, generative design, and design for manufacturing. Terms related to metal AM included "additive manufacturing," "laser powder bed fusion," and "directed energy deposition." AI and ML terms included "machine learning," "deep learning," "convolutional neural network," "recurrent neural network," "long short-term memory," "Gaussian process regression," "surrogate model," and "physics informed neural network."

To more specifically capture defect detection literature, we used terms such as "in-situ monitoring," "melt pool," "melt pool imaging," "porosity detection," "lack of fusion detection," "keyhole detection," "spatter detection," "optical tomography," "pyrometry," and "acoustic emission." For capturing the surrogate modeling literature, we used terms such as "thermal history prediction," "melt pool prediction," "residual stress prediction," "3D CNN surrogate model," "BiConvLSTM surrogate model," "operator learning AM," "neural ordinary differential equation," and "digital twin." Generative design searches included "generative design," "topology optimization," "generative adversarial network," "variational autoencoder," "diffusion model," and "reinforcement learning topology optimization." To identify design for manufacturing work, we used terms such as "design for manufacturing," "design for additive manufacturing," "manufacturable design," and "geometry modification." We also used abbreviations and keyword variants in our searches. Articles were included if they applied AI or ML to metal AM processes (PBF and DED), provided validated results (experimental, sensing-based and simulation-based), and represented influential and emerging research directions within one of the four focus areas of this paper. Our goal was not to conduct an exhaustive systematic search, but to curate high quality and illustrative examples that demonstrate current capabilities and trends in AI/ML for metal AM across defect detection, surrogate modeling, generative design, and design for manufacturing.

2 Defect detection

2.1 Metal AM processes

Powder Bed Fusion (PBF) and Directed Energy Deposition (DED) are the most common metal AM processes and will be the focus of this paper. In PBF, a high-energy laser or electron beam selectively fuses powder particles by melting part cross-sections layer by layer in a powder bed to fabricate a part. PBF is characterized by high resolution, good shape detail capability, but limited part size due to the size limitation of the powder bed. In contrast, DED involves blowing metallic powder (called powder-blown DED) or feeding wire (wire-fed DED) into a melt pool generated by a focused energy source. Since DED processes do not require a powder bed, much larger parts can be fabricated, although typically feature solution is limited; as a consequence, parts tend to be of limited complexity compared to PBF. Both processes offer the capability to fabricate complex, near-net-shape parts with tailored material properties. However, defects often occur, such as porosity, lack of fusion, cracking, and keyholing, as well as rough surfaces. Various in situ sensors and post-fabrication inspection techniques are used to identify these defects and to characterize their potential severity.

2.2 Defect detection technologies

Defect detection in PBF and DED processes is complicated by the stochastic nature of powder spreading, melt pool dynamics, rapid solidification, and thermal gradients. Although X-ray computed tomography (CT) and ultrasonic testing are effective in inspecting parts, they are costly and time-intensive, making them difficult to use for 100% inspection. Instead, in-situ monitoring during part fabrication is a promising approach for defect detection. Typical sensors in commercial machines include optical and infrared imaging using high-speed cameras or optical tomography,

photodiodes and pyrometers for point-wise, high-speed monitoring, acoustic emission monitoring using microphones or piezoelectric sensors to "listen" to the process, particularly for DED, and layer-wise height mapping using structured light or optical profilometry [8]. Table 1 summarizes the common sensors and the potential defects that they can detect, along with some representative references.

In PBF, scan speeds can be up to meters per second. For the best porosity detection capability, it is necessary to monitor the melt pool, which must be accomplished very quickly. For this, pyrometers that are coaxial with the laser are typically employed. Their limited field of view is acceptable since melt pools are small, on the order of tenths of millimeters in size [9, 10]. An approach using two pyrometers that sense at different wavelengths, known as dual wavelength pyrometry, can be used to estimate temperatures, as well as melt pool size and shape, since the use of multiple wavelengths corrects for uncertain emissivity of the melt pool region. Huge datasets are typically generated since melt pool monitoring requires millisecond time resolution and parts typically have many kilometers of scan vectors. By monitoring the melt pool, estimates of keyhole and lack of fusion porosity can be made [11, 12].

High-speed visible imaging is utilized to capture spatter rates, ejection direction, and plume unsteadiness, which are signatures of melt pool instability and powder denudation related to porosity risk [13]. When combined with schlieren and synchrotron X-ray imaging, the transition from a steady to a chaotic plume aligns with deeper, oscillatory keyholes and marks conditions that are prone to keyhole-driven porosity [14]. Optical tomography provides layer-wise intensity maps across the full build area, and persistent bright and dim bands together with simple geometric indices illustrate lack of fusion bands, short tracks, surface roughness, and dimensional deviations [15–17]. Layer-wise height mapping, for example, fringe projection profilometry, reconstructs a three-dimensional surface and height in each layer to show warpage, edge lift, and spatter deposits that drive lack of fusion and dimensional errors [18–20]. Acoustic emission is most sensitive to discrete release events such as crack initiation and powder and laser interactions. Regime classification comes from spectral features like band energy ratios and centroid frequency. Static pores are mostly quiet, but transitions into keyhole mode and pore formation or healing can generate bursts [21].

For DED, scan speeds are much slower and melt pools are typically larger, making real-time defect detection easier. Coaxial and dual wavelength pyrometry are often employed, as well as IR and visual wavelength cameras. Infrared cameras are utilized to track melt pool geometry and vertical displacement because drifts in pool area or centroid and layer height deviations at thin walls and turnarounds indicate porosity is likely, that is often corroborated by micro CT

Table 1 In-situ monitoring technology and defects detected

Sensor type	Data collected	Defects detected	Processes	References
Infrared camera	IR and X-ray images	Keyhole, bubbles, vapor plumes, surface depressions, bulges, and lack of fusion porosity	PBF, DED	[22, 26, 27]
Coaxial pyrometer	Emissivity signals, melt pool images, temperatures, and histograms	Porosity, density, cracks, lack of fusion, by-products of the melt pool, deformation, and balling	PBF	[9, 10]
Dual wavelength pyrometer	Emissivity signals, temperatures, melt pool images, thermometry images, histograms, and heat maps	Porosity, pore size, lack of fusion, cracks, contour deformation, spattering, and powder spreading anomalies	PBF, DED	[11, 12]
High-speed optical camera	Visible images of melt pool and spatter, thermal images, morphology maps, X-ray and schlieren images, photodiode signals, and modelling data	Spattering, porosity, lack of fusion, balling, surface roughness, powder denudation, and poor bonding from non-uniform melting	PBF, DED	[13, 14, 23]
Optical tomography	Layer-wise intensity maps (near-IR or visible)	Porosity, lack of fusion, surface roughness, geometric distortions, dimensional inaccuracies	PBF	[15–17]
Layer-wise height mapping (structured light & profilometry &interferometry)	Fringe projection images	Warpage, edge distortions, super-elevated edges, spatter deposits, and porosity	PBF	[18–20]
Acoustic emission (microphone & piezo sensor)	Acoustic emission signals (airborne via microphone, structure-borne via piezo sensor)	Porosity, cracks, thermal expansion bursts, powder interaction effects, and lack of fusion	PBF, DED	[21, 24, 25]

[22]. High-speed visible imaging of the powder stream and plume can capture laser beam shadowing and attenuation by the powder jet, glowing or partially vaporized particles, and impact cratering. All of them indicate nonuniform melting and weak bonding [23]. Acoustic emission monitoring using an airborne microphone or contact sensor records time lagged high frequency bursts from crack initiation and growth behind the laser path, enabling layer by layer crack detection [24, 25].

In-situ monitoring of metal AM has developed significantly in recent years, but several limitations persist. These include line-of-sight constraints, uncertainties in emissivity and calibration, sensitivity to noise and equipment setup, and the fact that sensor data only correlate indirectly with the actual defects. Large amounts of data generated also create challenges for real-time processing and analysis. Current research efforts focus on spatiotemporally coordinated multi-sensor fusion, the integration of physics-based and AI models for defect detection, online algorithms for emissivity and temperature calibration, and improved denoising and feature extraction techniques.

2.3 Machine learning techniques

The ML techniques used for defect detection include both conventional and deep learning approaches and depend to some extent on the AM process. ML algorithms can leverage multimodal process data, including optical imaging, thermal signals, and acoustic emissions, to automatically identify defects during or immediately after the build. This data-driven approach can lead to predictive quality assurance and lay the foundation for closed-loop control systems in AM. Reference [4] is a good review article focused on defect detection in metal AM processes, while articles [5–7] provide good introductions to the ML techniques often used in defect detection and other AM processes.

In PBF processes, defect formation is strongly tied to melt pool instabilities and powder distribution. In the continuous material deposition regime of DED, melt pool fluctuations caused by complex interactions between blown powder and the melt pool in powder blown DED and arc instabilities in wire-arc DED can cause defects.

ML techniques can be classified broadly into four categories for PBF and DED. In the first, supervised learning refers to conventional ML techniques that are trained using input-output pairs. Support Vector Machines (SVMs) and Random Forest classifiers have been used to detect lack-of-fusion porosity by analyzing thermal and optical sensor data [28]. These models use engineered features such as melt pool area, aspect ratio, intensity variance, and spatter counts. The identification of suitable features remains a critical aspect to the success of these ML techniques. Although these models are computationally efficient and interpretable, their accuracy is limited by training data quality and how well they represent the breadth of processing conditions.

The second category, deep learning, uses neural networks to enable more sophisticated reasoning from sensor data. Specifically, convolutional neural networks (CNNs) have shown great promise in detecting various forms of porosity and other defects by processing high resolution images. A major advantage of CNNs over conventional ML methods is that CNNs can learn discriminative spatial features from melt pool or powder bed images without manual feature design. Specific studies have demonstrated CNN-based identification of keyhole and lack of fusion porosity, balling, and recoater streaks with accuracies exceeding 90% [29, 30]. Reinforcement learning (RL) approaches have achieved success in adaptive deposition path control in DED, enabling correction when ML models predict bead height inconsistencies [31]. They have also been proposed for multi-parameter control that adjusts process variables such as laser power, laser spot diameter, scan speed, and powder flow rate in both PBF and DED. In this framework, anomaly detection automates the reward signal, enabling the controller to dynamically respond to process variations and prevent defect propagation [32].

Another class of deep learning techniques is temporal models such as recurrent neural networks (RNN) long short-term memory (LSTM) networks. These models operate by processing time series data to capture sequential dependencies. For AM processes, this means that the periodic sensor readings are analyzed to capture melt pool dynamics and, in many cases, can predict the onset of pores and other defects. Hybrid CNN-LSTM models have been applied successfully as well. For example, Cannizzaro et al. [33] used an LSTM autoencoder for real-time anomaly detection in PBF, while Pandiyan et al. [34] developed a hybrid CNN-LSTM framework for PBF regime classification (lack of fusion, conduction, keyhole) and validated with operando X-ray imaging.

Used primarily with DED, acoustic and vibration-based detection approaches construct distinct acoustic signatures correlated with defects such as porosity and lack of fusion. Supervised learning methods such as decision trees and SVMs have been trained to classify acoustic emission signals, achieving reliable defect detection without visual monitoring [35, 36]. To enable classification, wavelet transformations and spectrogram-based features are commonly extracted [35, 37].

Finally, multi-sensor data fusion approaches combine several sensor readings to reach a more comprehensive understanding of melt pool dynamics, process conditions, and part characteristics [38]. DED defect detection benefits from multi-sensor fusion frameworks where thermal, acoustic, and optical data are jointly analyzed [39]. Ensemble learning and probabilistic models integrate heterogeneous features to improve detection reliability. This is particularly valuable

in industrial settings where sensor noise or occlusion can reduce the accuracy of single-sensor methods. Besides that, a broader shift has occurred from CNN-only pipelines to graph-based, attention, and transformer architectures for multi-sensor fusion in PBF. Transformers are recognized as enabling latent-space alignment of heterogeneous data streams, making them strong candidates for future closed-loop control [40].

Significant challenges remain, including training data scarcity and labeling, generalization across machines and materials, real-time deployment, and interpretability. Some emerging solutions have been investigated, such as transfer learning to adapt models across different machines and vendors [41], unsupervised approaches to avoid the need for extensive labeled training datasets [42], and physics-informed machine learning to integrate physics models [43] and overcome limitations in purely data-driven approaches. Diffusion probabilistic models are also emerging as powerful tools for AM defect detection and quality assurance. They have been used to augment limited datasets with realistic synthetic defects, enhance sensor resolution and improve the detection of subtle anomalies [44, 45] (Table 2).

2.4 Examples

One example of defect detection in PBF is an unsupervised defect detection framework for identifying overheated regions and mechanical distortions. The approach integrates time-series analysis with image-based analytics from coaxial dual-wavelength pyrometers [47]. A CNN-based architecture converts sparse pyrometer data into feature-rich images for detecting overheated regions and part quality issues without relying on labeled training data.

Two examples were investigated to validate the framework: an overhanging cantilever and a bridge with an arch. Results demonstrated the method's capability to identify both global and localized defects, including cracks and overheating regions, which traditional time-series analysis may overlook. Additionally, the approach provides human-interpretable visual outputs, enabling operators to monitor the build in real-time, gain insights into the PBF process for a specific part, and explain findings to others. Some representative results are shown in Fig. 1, which shows the overhang cantilever part and processed layer images that indicate clear temperature differences between the column and overhang regions in the first cantilever layer.

A second example focuses on anomaly detection using a supervised learning approach, with an emphasis on porosity, in the DED of metal matrix composites (nickel-tungsten carbide (Ni-WC)) [46]. Dual infrared cameras provided the sensor data for deep learning feature extraction and processing. The approach taken is illustrated in Fig. 2. A dataset containing 80 videos of melt pools and laser-powder interactions in single-track deposition was prepared for training purposes. In stage 2, a CNN and transformer-based architecture was applied to learn features that indicate one of three states: normal, defective, and failure process states. Subsequently, the separate video feeds are processed to classify the extents of each anomaly type into three levels of absent, low, or high. Each class is then further processed to better detect the extent of each anomaly using cross-validation and hyperparameter search methods. In stage 5, the models from each camera type are fused in three different manners: direct feature fusion, decision-level fusion, and confidence-based fusion techniques. This multi-stage approach successfully recognized and classified six types of anomalies, including porosities, excessive dilution of the base, excessive dissolved carbide, non-uniform carbide distribution, and re-precipitation of hard phases. Additionally, the exploration of different camera types, ML techniques, and data fusion methods enabled identification of more effective approaches in each case. An important conclusion was that the dual-camera and data fusion approaches worked well since the strengths of one technique could provide a counterbalance for its weaknesses.

2.5 Discussion

Challenges associated with defect detection will be summarized, followed by a proposal for research directions. A wide range of ML techniques has been applied successfully

Table 2 Types of ML techniques for defect detection

ML type	ML techniques	Defect detection applications	References
Supervised learning with conventional ML	Support vector machines, Random forest	Lack-of-fusion porosity	[28]
Deep learning	Convolutional neural networks, Reinforcement learning	keyhole and lack-of-fusion porosity, balling, recoater streaks; bead height inconsistencies, process control	[29–32]
Temporal models	Recurrent neural networks, Long short-term memory	melt pool dynamics, porosity, spatter	[33–37]
Multi-sensor data fusion	CNN, Graph NN, Attention mechanisms, Transformers	melt pool dynamics, porosity, nonuniform precipitate distributions	[38–40, 46]

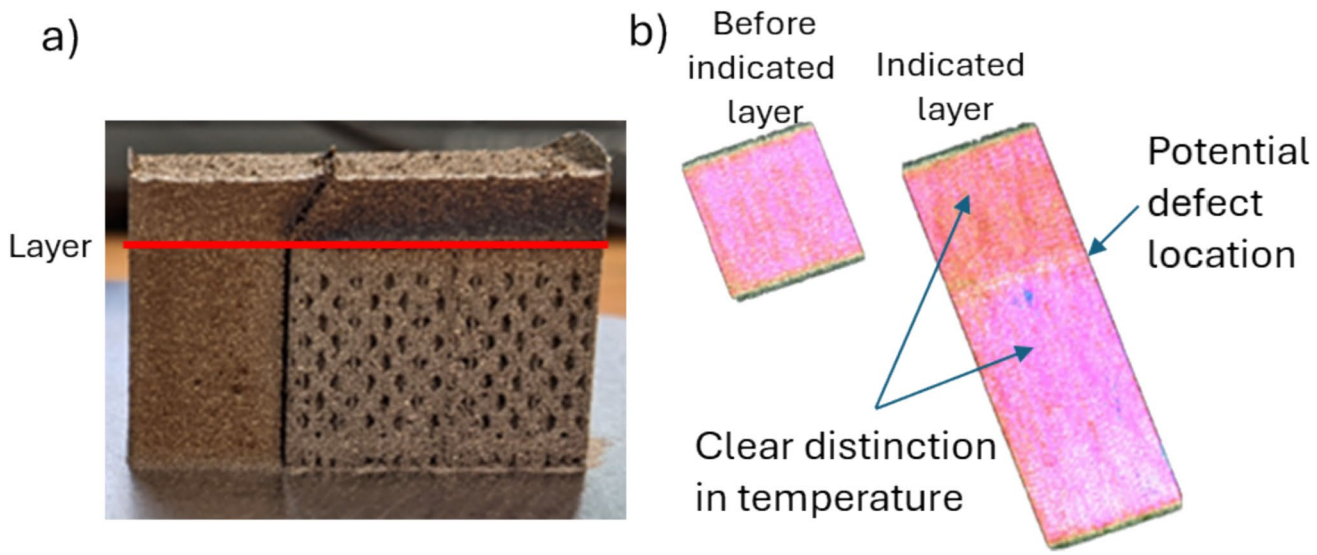

Fig. 1 Defect detection results from unsupervised learning of potential defect location due to overheating. **a** Part with crack initiated at start of cantilever section, with the first cantilever layer indicated. **b** CNN-based visualization of the last layer before the cantilever (labeled "before indicated layer") and the first cantilever layer showing temperature differences between the layer regions and the location of the potential crack defect

to the defect detection problem, from conventional ML to advanced deep learning methods. In one sense, a main challenge is to identify appropriate sensors and ML techniques for the specific type of defect to be detected. Many research works investigate a large number of ML techniques, then compare and contrast their capabilities, with many of the results showing that several techniques can work equally well. Perhaps the larger challenge is to develop defect detection techniques that work for all expected defect types in a given process, given that different defects are caused by different physics and appear at different size scales. This can necessitate the use of multiple sensors that, hopefully, work synergistically to efficiently detect a wide range of defects. A second challenge relates to the lack of generality of developed ML models. A defect detection tool that works for one material in one specific AM machine may not work well for a different machine, or machine vendor, and may fail badly for another material, particularly if the material has very different processing characteristics, such as stainless steel vs. copper. A third challenge arises due to the relative infrequency of defect occurrence. Data scarcity and imbalance are challenges that cause issues in developing high-quality training datasets. Taken together, the second and third challenges can lead to long defect detection system development efforts for a system that has only narrow uses.

Given these challenges (and many more), promising research directions can include methods that enable broader generalization and domain adaptation. Hybrid data-driven and physics-informed approaches may be successful here if the dominant physics of each defect type can be modeled and then tuned to the specific material, process, and machine of interest. Transfer learning approaches could help make models of the underlying physics generally applicable. Sensor fusion with uncertainty quantification methods could assist with the development of systems to detect a wide range of defects that achieves synergy, improves predictions, and estimates detection confidence. Finally, shared datasets and standardized metrics and benchmarks could help to alleviate challenges with scarce and imbalanced datasets while promoting research progress in the field. Different detection methods can be tested and compared consistently across defect types, materials, and processes.

3 Surrogate models and optimization of AM processes

In recent years, significant advances have been made in AM process simulation, particularly for metal AM processes. Powder-scale simulations are typically based on high-fidelity models that capture the relevant physical phenomena of laser-powder interactions, powder melting, melt-pool dynamics, and cooling and solidification processes. Phase-field models can be integrated to predict microstructures and, ultimately, mechanical properties. Part-scale simulations simulate the layer-by-layer fabrication process for an entire part using lower-fidelity models. Temperature distributions, thermal histories, residual stresses, and deformations are typical outputs of these models, which can be used to predict overheated locations, locations where cracks may

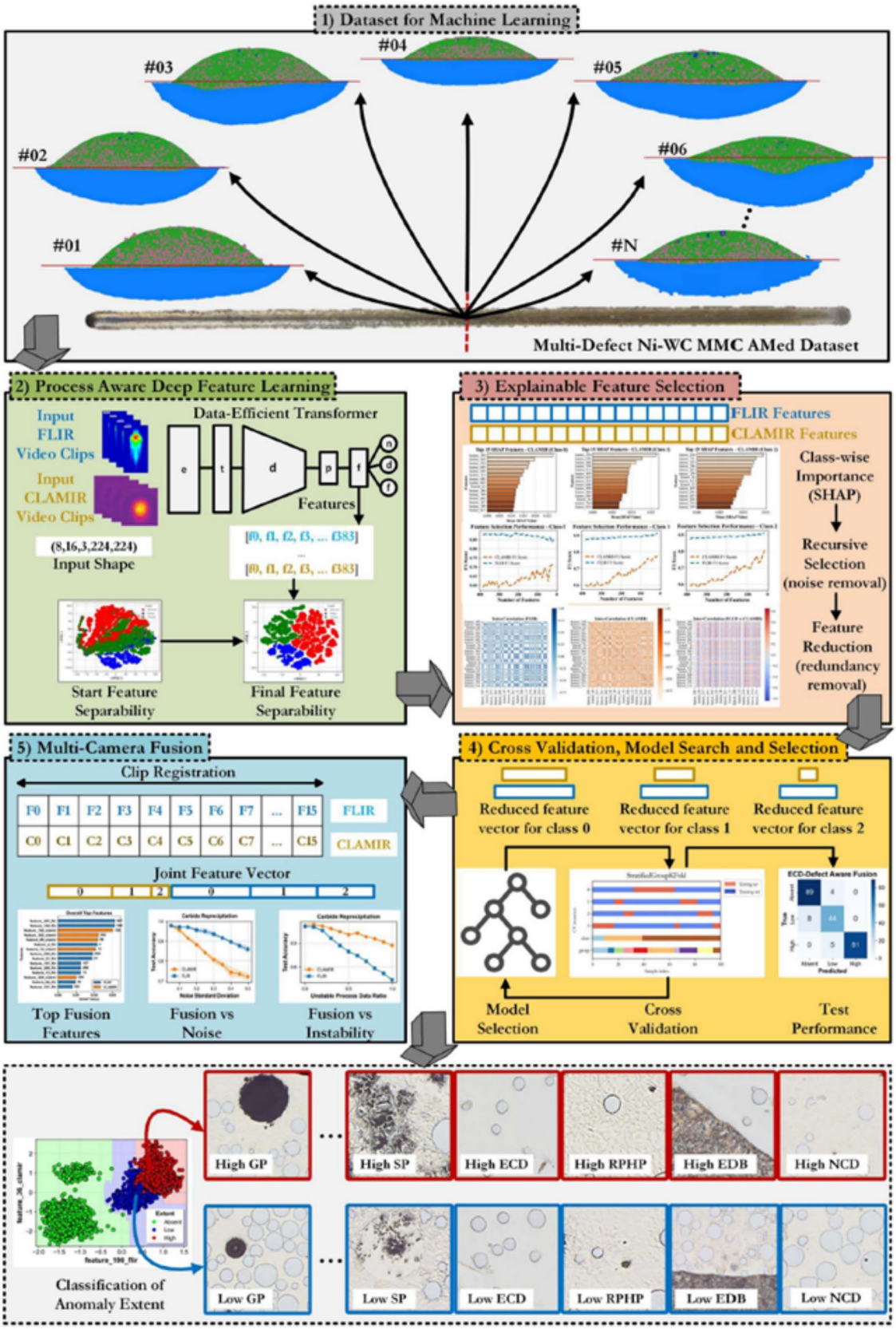

Fig. 2 Framework for multi-camera defect detection in DED of Ni-WC [46]

occur, and overall part accuracy. Some commercially available simulation software systems include ANSYS Additive, Simufact, and offerings integrated into mechanical CAD systems such as Siemens NX and CATIA from Dassault Systems.

A main challenge with process simulation is the computational complexity of the process models. Simulation times, whether for part-scale or sub-millimeter powder-scale simulations, often run for many hours (sometimes longer than a day) on standard computer workstations. Although such simulations can provide useful insights into part characteristics, computation times are far too long for process planning or part optimization purposes. Hence, researchers have investigated the use of surrogate models to replace simulations for these applications. An important application of these models is to optimize the AM process, which would be prohibitive if only high fidelity simulations were used.

3.1 Surrogate models

Data-driven methods and artificial intelligence have been used to build surrogate models to predict thermal fields, microstructures, material properties, etc. [48]. A Gaussian process regression (GPR)-based surrogate model quantified the grain size distribution of the microstructure which replaced an expensive FEA model [49]. GPR approaches have also been used to build surrogate models for process planning, such as predicting melt pool depth [50] or the temperature history [51] as a function of process variables. However, these studies were limited to single-track experiments, not to part-scale builds. Li et al. [52] proposed a physically based and data-driven approach to predict the thermal history of the PBF process using the GPR method with Bayesian calibration. Results showed that the thermal field can be determined quickly for different process parameters and geometry designs. Deep learning approaches have also been investigated, for example, an artificial neural network (ANN)-based surrogate model predicted thermal histories of the PBF process [53]. They directly translated a part's manufacturing G-code into a set of features instead of using the part geometry. Prediction errors were reported to be below 5%. Pham et al. [54] demonstrated an ANN surrogate model to predict temperatures and quantify uncertainties in DED, which accelerated Monte Carlo simulations by over 100-fold while maintaining accuracy. Except for Ref. [50], most existing research has focused on simple geometries.

To enable fast, accurate part-scale predictions, more sophisticated ML approaches are needed. Surrogate models for metal AM processes have evolved to capture multiple physics and scales, demonstrated the ability to generalize across diverse geometries and process conditions, and to increasingly incorporate physics-based constraints and uncertainty quantification in the past 3 years. Hemmasian et al. [55] developed a 3D CNN surrogate model with an enhanced auxiliary masking network to predict full melt pool temperature distributions in PBF. The model achieved a root mean square error below 5% and an intersection-over-union (IoU) score of 80–90%. Wu et al. [56] applied RNN surrogates, specifically LSTM, bidirectional long short-term memory (Bi-LSTM), and gated recurrent unit (GRU) models to DED. The Bi-LSTM achieved a coefficient of determination (R2) of 0.983 for peak temperature prediction, while the GRU reduced computational cost by about 30%. Lestandi et al. [57] introduced and compared interpolation, multilayer perceptrons (MLPs), and a U-Net CNN for residual stress prediction in PBF, all of which were thousands of times faster than the reference full-order model. The U-Net CNN provided the best generalization across geometries.

In addition, physics-informed neural networks (PINNs) [58] and hybrid operator-learning models [59] embedded the governing partial differential equations (PDEs) directly into surrogate training, enabling data-efficient, parametric solutions for single and multi-track processes. Parallel progress in DED includes multimodal CNN surrogates [60] that fuse scan path images with various process parameters, which achieve substantial accuracy and provide direct uncertainty quantification. Kannapinn et al. [61] developed autoencoder-based surrogate models combined with neural ordinary differential equations (NODEs) for integration into digital twins, enabling accurate real-time prediction of temperature and residual stress fields to support process control in DED. Peng et al. [62] introduced an eXtended Physics-Informed Neural Network (XPINN) framework to predict DED thermal histories by decomposing the domain spatially and temporally with a trained subnet per sub-domain, targeting realistic scenarios such as interpass time, voids, and scan interruptions. Overall, these works illustrate clearly that surrogate models in metal AM have become faster, more accurate, and more generalizable, enabling real-time prediction, uncertainty quantification, and integration into digital twins and process control for both PBF and DED.

Research on ML techniques used for surrogate modeling is summarized in Table 3, which covers the contents of Sect. 3.

3.2 Examples of surrogate models

Two examples of CNN-based surrogate models will be presented to illustrate the potential of deep learning approaches. The first example used a feature-based approach in that a dataset consisting of part features of various shapes, sizes, and combinations was used for training [69]. The idea is that if parts are encountered with similar features, the surrogate model will successfully predict their characteristics. In this case, basic features such as struts and walls were used to generate a large set of training geometries. Each

Table 3 ML research on surrogate modeling and usage in process optimization

ML type	ML techniques	Surrogate modeling applications	References
Supervised learning with conventional ML	Gaussian process regression (GPR)	Microstructure grain size distribution	[49]
	GPR	Predict melt pool depth, temperature history, thermal history (PBF)	[50–52]
	Support vector regression (SVR)	Thermal histories to optimize PBF processes	[63]
	GPR	Melt pool temperatures to optimize PBF processes	[64]
	K-means clustering, SVR, GPR, Random Forest	Optimize PBF processes to maximize strength and ductility	[65]
	SVM, Decision Tree (DT), KNN, GPR, ANN	Mechanical properties	[66]
	Artificial neural network (ANN)	Thermal history (PBF)	[53]
	ANN	Temperature distributions and variations (DED)	[54]
	ANN and PSO	Minimize energy consumption (PBF)	[67]
	RSM, ANN, and evolutionary optimization	Optimize PBF process to maximize density	[68]
Deep learning	3D CNN	Melt pool temperature distributions (PBF)	[55]
	3D CNN, MLP	Residual stresses in PBF	[57]
	3D U-net CNN	Deformations and residual stresses in PBF	[69]
Temporal models	RNN, Bi-LSTM	Peak temperatures in DED	[56]
	Bi-LSTM w/CNN	Residual stresses in PBF	[70]
Physics embedded in neural networks	PINN	Temperature distributions (single or multiple track PBF)	[58, 59]
	PINN	Temperature distributions (DED)	[60]
	Autoencoder + neural ordinary differential equations	Temperature and residual stress fields (DED)	[61]
	Extended PINN (XPINN)	Thermal histories (DED)	[62]

was simulated using a high-fidelity PBF process simulator to generate the training data [71]. The surrogate model architecture was a 3D U-Net CNN, since this has a good capability to learn abstract features directly from voxelized geometries without requiring explicit parameterization. With the U-Net architecture design, our model produces output values for each input voxel, allowing it to predict part properties throughout the part.

The 3D U-Net CNN was trained with about 900 distinct models consisting of combinations of flat and cylindrical walls and round and square struts of various sizes, positions, and orientations. Data augmentation, copying the inputs and outputs for different orientations and positions, so that the training data set consisted of about 3600 input-output pairs.

Results demonstrate that the CNN model can accurately predict residual stresses and deformations in PBF fabricated parts. The CNN model has good shift and rotational invariance properties as a result of the augmented training data approach. Four benchmark parts tested the residual stress and deformation prediction capabilities of the CNN model, which are shown in Fig. 3a. These parts consisted of features similar to those in the training dataset, but with more features and more complex feature interactions. With the increase of part complexity, prediction accuracy on the benchmarks was lower than for the testing data as shown in Fig. 3b. However, the overall stress distributions and locations of stress concentrations were predicted accurately.

The second example utilized a more sophisticated type of ML architecture for PBF surrogate modeling. A bidirectional convolutional long short-term memory (BiConvLSTM) approach was used to enable predictions of residual stresses [70]. LSTM models are used typically for series data, such as streaming sensor data, audio, or video. The key insight was that the series data that justified the use of an LSTM approach was the layer-by-layer fabrication process of PBF. That is, the sequence of layers formed the series data that the BiConvLSTM processed. The model architecture is shown in Fig. 4, where the inputs were voxel models of the part and the base (build platform). The outputs were the predicted residual stresses and variances for each voxel in the part and the base.

Results are shown in Fig. 5 for four parts, two cantilevers and two sizes of a jet engine bracket. Each column in the figure represents a source of the residual stress predictions. The left column shows the ground truth from the finite element analysis (FEA)-based PBF simulator. The second column

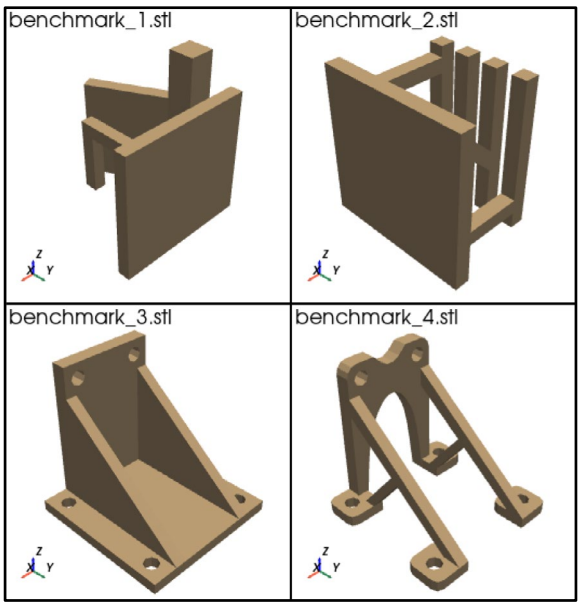

a) benchmark parts

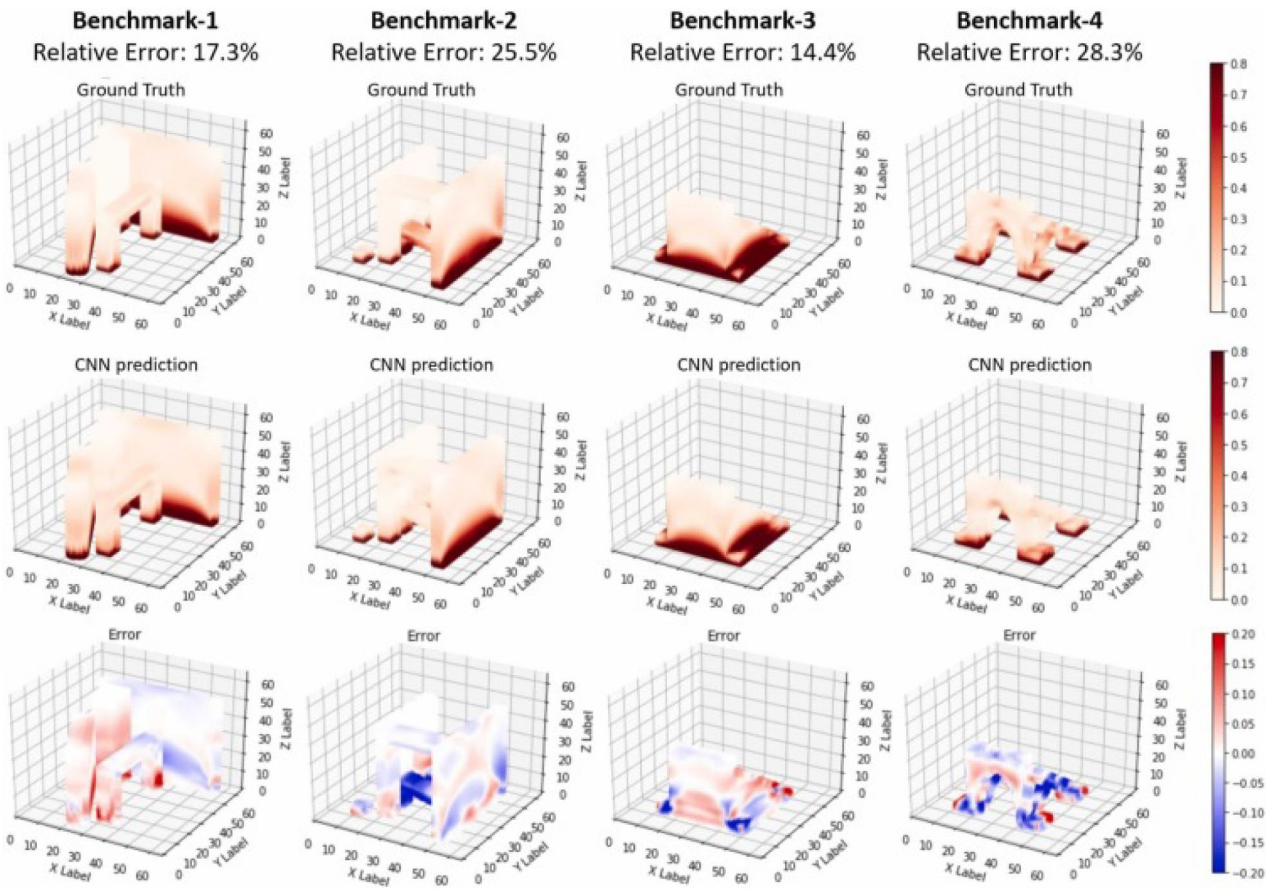

b) residual stress distributions: ground truth as computed from the PBF simulation (top), CNN predictions (middle), and prediction errors (bottom) for the four benchmark parts

Fig. 3 Benchmark parts and the results of applying the 3D U-Net CNN for the prediction of residual stresses [69]

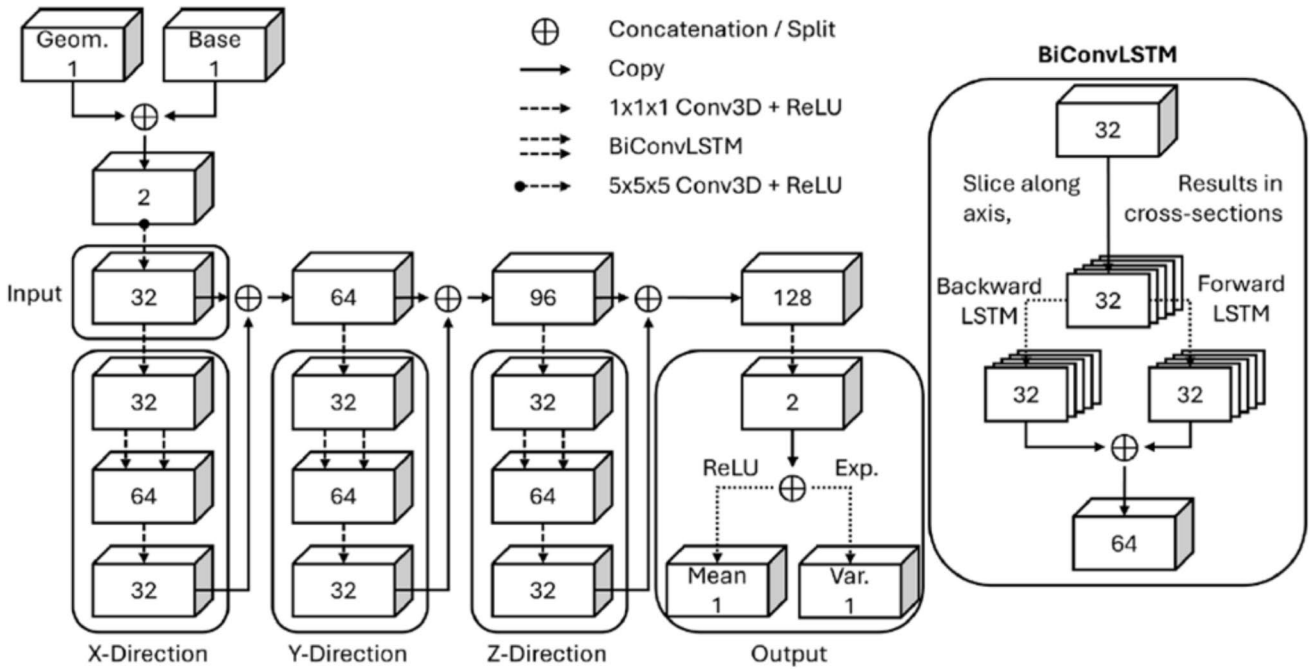

Fig. 4 Architecture of the BiConvLSTM surrogate model [70]

shows stress prediction results from the U-Net-based predictions from [69], while the 2 right-hand columns show results from the BiConvLSTM model. Although all predictions exhibit the residual stress trends shown in the FEA ground truth results, the BiConvLSTM predictions appear to more closely match the ground truth than the U-Net-based predictions. The superior prediction capabilities of the BiConvLSTM approach are most clearly visible in the jet engine examples.

Surrogate model prediction capabilities are dependent on many factors, but principally they relate to the training dataset and the inherent capabilities of the ML architecture. The capability of the BiConvLSTM technique to learn from the layer-by-layer fabrication process seems to be an advantage of that approach. Also, the dataset used to train the U-Net model consisted of thin walls and struts, which is not well matched to the jet engine model that was used for testing.

3.3 Process optimization

A common application of surrogate models is to improve or optimize the AM process. A good review article on AM process optimization for papers published to 2023 is provided in [72]. In each case, they identify process-signature-structure-property relationships captured by the surrogate models, and then categorize the ML models used into three classes: interpretable ML, conventional ML, and deep ML, which are given in order of increased accuracy and complexity. Interpretable ML techniques are the simplest to apply and understand; they include linear and logistic regression, as well as decision trees and other regression and rule-based techniques. Conventional ML techniques include support vector machines, artificial neural networks, random forest, Gaussian process, and K-means clustering, while deep ML encompasses deep neural network techniques such as CNNs, RNNs, deep forest, and autoencoders.

Most of the work related to this topic involved the authors applying ML techniques to model relationships among process settings, process signatures (e.g., melt pool characteristics), material microstructure, and physical properties (e.g., density, strength) with the objective of maximizing model accuracy. Some researchers used the methods to identify preferred process settings, while a small number applied optimization algorithms, using the model instead of high-fidelity simulation, to determine the best process settings.

An interesting usage of a process signature was the work of [63] who used support vector regression to relate process parameter settings to local thermal histories for different local part geometries. They used principal component analysis and partitioning to perform dimensionality reduction to form a reference parameter-thermal history map. This map can be used for the multiobjective optimization (objectives were to match local thermal histories and minimize scan time) of the PBF process for a given part geometry. The authors demonstrated the method with Ti6Al4V material on several simple part geometries with success.

An example usage of surrogate models for process optimization was reported by [64] who modeled melt-pool

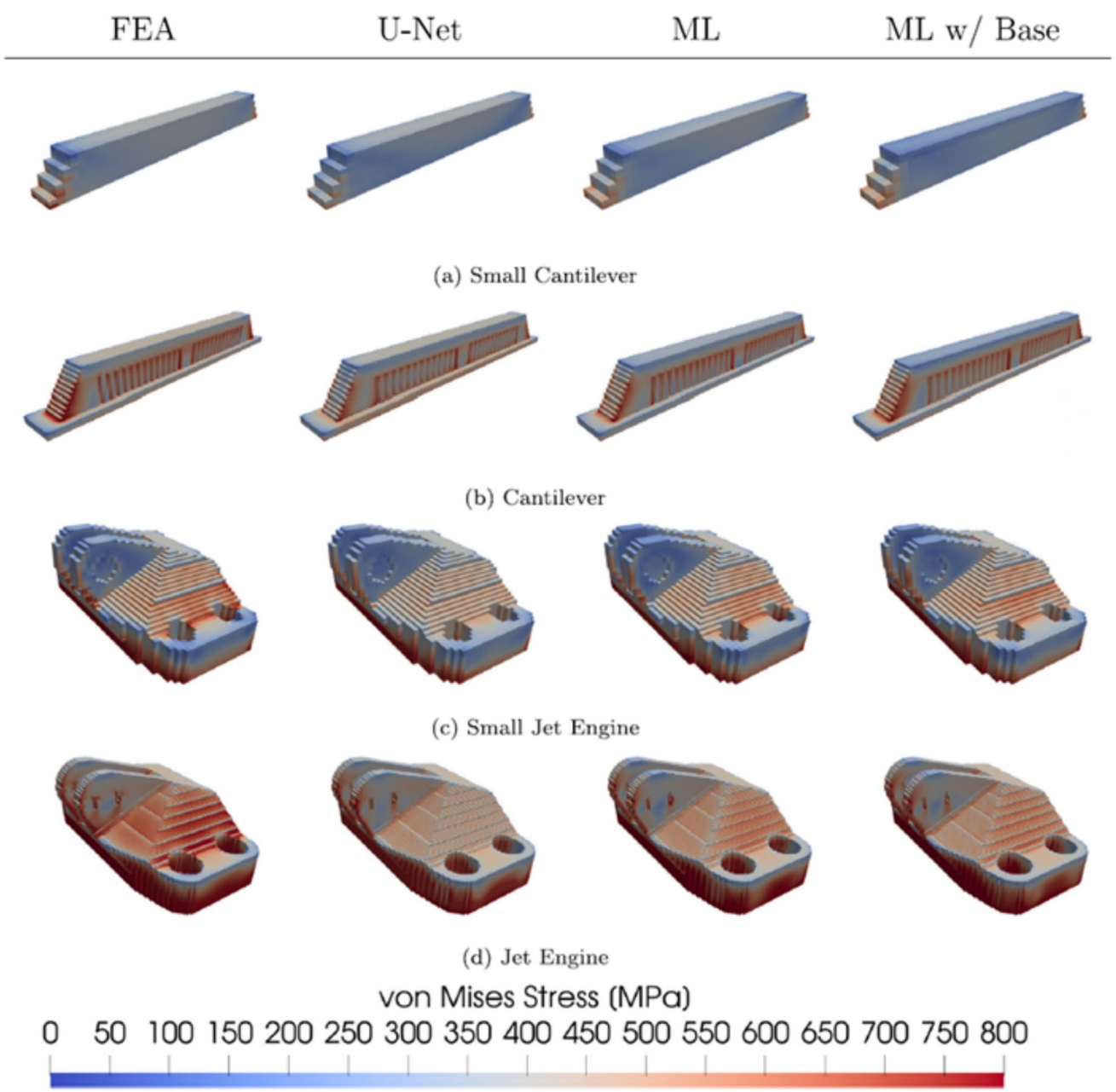

Fig. 5 Results showing a comparison of the U-Net-based [69] and BiConvLSTM-based [70] surrogate models with the ground truth (FEA column)

dynamics in PBF. They used GPR to relate process settings to melt pool temperatures. Then they used the GPR model in a projected gradient descent algorithm to determine laser powers for multiple tracks to regulate the melt pool size in an off-line manner.

A research group employed deep learning techniques for surrogate modeling and particle swarm optimization (PSO) to minimize energy consumption during the fabrication process [67] for polymer PBF. Input data for their deep ANN included part measures (part size, % of powder bed filled by parts, etc.) and process settings and was obtained from 2 years of usage involving more than a hundred builds and thousands of parts. They investigated three different problem settings that emphasized designer objectives, manufacturer objectives, and a balance of all objectives.

Another research group investigated response surface methodology (RSM) and ANNs to model the relationship between PBF process variables and part density [68]. Then, they employed three evolutionary optimization methods (self-adaptive harmony search, genetic algorithm, and

particle swarm optimization) to identify the best process settings. Results showed that all three optimization algorithms were effective, although the authors preferred the self-adaptive harmony search. Additionally, the ANN model was superior and predicted smaller laser power and scan pattern angle values and higher hatching values than the RSM model.

Some researchers have used surrogate models and optimization to obtain superior mechanical properties. One example was to simultaneously enhance the strength and ductility of Ti6Al4V fabricated using PBF through process-structure-property relationships [65]. The researchers applied K-means clustering on data on yield strength, ultimate tensile strength, and elongation at break from the literature to group process-property relationships into 3 clusters for each property. Then they tested three ML models on each cluster to determine which model was best for each cluster for each property. The best models were combined using a technique called the cluster-integrated regression model (CIRM) to predict the properties. A genetic algorithm was used to search the models to identify process settings that yield the desired combinations of strength and ductility. Of interest, the authors identified that adjusting the grain size of martensite through process parameters can enhance both properties. A similar study tested several conventional ML models (SVM, DT, KNN, GPR, etc.) with ANNs to predict mechanical properties as a function of process variables [66]. The authors found that the ANN was superior in capturing the complex process-property relationships.

3.4 Discussion

Similar to the discussion on defect detection, challenges related to surrogate modeling are related to the complex physics of metal AM processes and limitations of training datasets. Again, a wide range of ML techniques has been applied successfully for surrogate modeling. But they tend to be expensive and time-consuming to build using either (or both) experimental or synthetic (modeling) datasets. Relationships between process variables and responses, such as residual stress, thermal history, and deformations, tend to be specific to the process and material being modeled and, to some extent, machine-specific as well. Furthermore, the relationships can be highly related to part or feature geometry as well. Taken together, surrogate models tend to be of limited applicability. Furthermore, many surrogate models capture input-output relationships without consideration of the underlying physics or path dependence and cannot adapt when process conditions cause unmodeled physical phenomena to become prominent. Stated differently, most surrogate models can interpolate well in well-modeled regions, but degrade quickly when extrapolating. Particularly when optimizing a process, it is important to utilize only those regions of the process modeling space where the surrogate model is known to give accurate results.

Given that surrogate models tend to suffer from a lack of physics understanding, weak extrapolation ability, and limited interpretability, future research directions should address these shortcomings. Hybrid data-driven and physics-informed approaches should be pursued that can enhance the applicability and generalizability of surrogate models. A multi-scale approach should be investigated that captures and integrates process behaviors across size scales. Bayesian and related sampling methods could be investigated to identify regions of the process modeling space that are under-represented or require additional model accuracy. Based on the comparison of example methods in Sect. 3.2, the issue of temporal process modeling should be investigated; that is, does modeling the layer-by-layer nature of the AM process yield a more accurate process model? Or is it sufficient to model only the final physical state of the fabricated part? This question raises related issues regarding the computational and experimental expense of developing training datasets, as well as their fidelity.

4 Generative design

The term "generative design" (GD) has several meanings that depend on the context. Most generally, GD refers to a methodology where the designer defines a problem and establishes the design space, rules, and constraints for the problem, then an automated or semi-automated system generates designs accordingly. In engineering design, GD technologies are typically used for early-stage conceptual design and can be classified into two approaches, one based on commercial computer-aided design (CAD) tools and mathematical problem formulations, and one that is based more on AI that is not based solely on mathematical optimization problems. These two techniques will be explored further in the next two subsections. The relationship to AM is that the designs produced are often geometrically complex, necessitating the use of AM processes for their fabrication.

4.1 Commercial tools

At present, generative design tools in commercial CAD tools define design problems mathematically as optimization problems and solve them using a combination of ML and optimization methods. For example, a structural design problem would be formulated by setting up a structural FEA model with a simple shape for which the final design is desired, then specifying objectives and constraints. That is, the designer specifies a geometric design domain and applies loading and boundary conditions that represent the structural problem. Depending on the tool, the design objective may

be specified as minimum weight, maximum stiffness, uniform stress, or even cost. Most commercial tools allow the designer to select a material and a manufacturing process such as 3-axis machining, casting, or additive manufacturing. They also support the formulation and solution of thermal, fluid flow, or multi-physics problems.

Using a combination of topology optimization (TO), evolutionary search algorithms, and ML techniques, the GD tools can generate a wide range of designs which the designer can then explore and identify those that appear promising for further development. If AM or no manufacturing process was specified, then resulting designs tend to resemble those from topology optimization, with complex, curved organic shapes. If, for example, 3-axis machining was selected, resulting designs will tend to consist of block-like features that are oriented relative to one another to minimize the number of machining set-ups.

Autodesk was the first CAD vendor to develop GD tools, which are now offered through their Fusion 360 platform. They offer a wide range of multiphysics problem formulations and have particularly strong capabilities for design for manufacturing processes. The other major CAD vendors, Dassault Systemes, PTC, and Siemens offer GD tools through their CATIA, Creo, and NX systems, respectively. All tools utilize cloud computing to off-load the high computational demands of GD from the designer's workstation. nTopology is another CAD vendor that offers GD capabilities, albeit using a different approach and different technologies. Their software enables reusable workflows to encode user-defined optimization logic with integrated lattice structure or minimal surface constructs and field-driven topology approaches.

4.2 Research frontier

Engineering design researchers have explored the application of emerging AI/ML technologies to develop GD capabilities that go beyond what is available commercially. For our purposes, we will view GD research as based on topology optimization. [73] classified research on ML in TO into 7 main purposes. From a coarser perspective, however, two primary directions can be considered. In the first, the objective is to improve the computational efficiency of TO methods. The second is to generate a very wide range of designs using ML techniques, coupled with engineering analysis or optimization tools to ensure that designs satisfy engineering requirements. Several deep learning techniques have been applied to GD, including generative adversarial networks (GANs), variational autoencoders (VAEs), reinforcement learning (RL), and diffusion models (DM). Some representative works will be summarized in each of the GD directions indicated here.

Research to improve the efficiency of TO generally seeks to avoid the iterations that require time consuming finite element analyses of intermediate solutions. Perhaps the simplest approach is to use training data sets consisting of initial problem descriptions paired with final TO solutions, enabling the ML model to learn how to avoid the TO iterations. That is, the initial problems consisted of the initial geometric domain with loading and boundary conditions applied and the target volume fraction specified. Abueidda et al. [74] used this approach for 2D problems using a CNN to predict optimized shapes. They trained models for three types of material characteristics, including linear elasticity, material nonlinearities (hyperelastic response), and geometric nonlinearity. Sharpe and Seepersad [75] utilized a conditional GAN (cGAN), instead of a CNN, to solve similar problems. Rawat and Shen [76–78] published a series of papers applying the Wasserstein GAN for 2D and 3D problems to predict both the optimal shape but also the optimization conditions (volume fraction, penalty, smoothing filter radius). Zheng et al. [79] demonstrated a 3D CNN that predicts TO results and employed a novel adaptive sizing model to accommodate problems with variable geometric domain sizes.

To achieve better results, other researchers introduced physical fields into the input models of their training datasets. For example, Zhang et al. [80] first performed an FEA to find the strain field in the starting geometric domain and included it in their training data for their CNN model. Similarly, Nie et al. [81] used strain energy density and von Mises stress distributions obtained from FEA as inputs to their cGAN system. Deng et al. [82] took a different approach in that they used a CNN to predict objective function values, rather than relying on FEA for these predictions. In this manner, they did not avoid TO iterations, but they were very fast. Chen et al. [83] trained a neural TO model but injected the initial strain-energy field from an FEA model of the unoptimized domain as an extra input, which sped up convergence and improved quality versus ML without physics conditioning. Seo and Kapania [84] developed a U-Net surrogate model that used results from an initial static analysis (mapped physics fields) as inputs and predicted the optimal layout in one forward pass, avoiding iterative solves. Yan et al. [85] used the initial principal-stress field from a quick FEA model into a U-Net model so it could directly predict the optimal topology (near real-time) without iterative solves.

Another approach to improve designs was to use a multistage approach, that is, to use sequential models, one for estimating an intermediate design from the initial conditions and the second for predicting the final optimized shapes from the intermediate design. Yu et al. [86] utilized a CNN-based model to generate low-resolution models as a first step. Then a GAN converted the low-resolution models into high-resolution solutions. In the thermal domain, Li et al.

[87] applied a similar two-step approach using two GANs to predict high-resolution solutions.

To generate a wide variety of designs, most approaches utilize an ML model for generation, then TO to modify the generated designs to ensure that they meet engineering requirements. Typically, this is an iterative process where the results of TO are fed back into the ML model to generate more design variants. An early example of this approach was by Oh et al. [88] who solved a 2D wheel design problem using a GAN to generate designs and TO to ensure structural requirements were met. Wang et al. [89] proposed a novel approach that embedded TO into the GAN model by adding terms to the GAN's loss function that represented compliance minimization (the TO objective function) and the volume fraction constraint. They demonstrated that their approach could generate at least as many designs as the Oh et al. model [88] for the same wheel design problem, but with far fewer iterations. Other work utilized RL to maximize diversity and aesthetics. Jang et al. [90] utilized two neural networks, one that replaced TO and the other to find design parameter combinations that maximized diversity. Yet others explored the use of VAEs. For example, Yamasaki et al. [91] implemented a multiobjective structural TO method pairing a VAE with conventional TO to generate new material distributions. Extensions to 3D have been demonstrated for GD as well. Shu et al. [92] presented a GAN model that generated aircraft models and evaluated them using complex computational fluid dynamics simulations. Mazé and Ahmed [93] introduced TopoDiff, a conditional diffusion approach guided toward low-compliance and feasible structures. This model outperformed a cGAN baseline and reduced unmanufacturable outputs. Chen et al. [94] presented a neural framework that co-optimized topology, build orientation, and support part segmentation to minimize supports for additive manufacturing, incorporating print-setup decisions inside the design loop. Kumar et al. [95] used an RL (PPO) agent that interacted with an FEA loop to add or remove material under stress ($\leq$300 MPa) and displacement limits. After optimization, Signed Distance Function (SDF) smoothing was applied to the resulting design and an STL could be output for printing.

5 Design for manufacturing

Design for manufacturing (DFM) refers to the modification of part geometry to avoid manufacturing problems (e.g., eliminate an undercut in injection molding) or to facilitate an aspect of a manufacturing process (e.g., change feature orientations to reduce the number of set-ups in machining). Relatively little research has applied AI/ML techniques to DFM compared with many other engineering topics. In this section, three approaches to DFM will be offered. The first is to combine an ML technique with an optimization model, such as TO, while the second uses neural networks to model scalar fields that model structural and manufacturing design spaces in a co-optimization framework. The third illustrates how GANs can be used to directly modify part representations in the form of pixel images and voxel models.

5.1 Combination of ML and optimization

Building on the multi-scale gradient structure GAN (MSG-GAN) [96], Greminger et al. [97] generated,3D manufacturable designs from a TO problem formulation for the 3-axis machining process. The trained MSG-GAN was embedded in the TO algorithm by using the latent feature vector (input to the GAN) as the design variable, rather than element densities. Element densities were predicted by the GAN. The GAN model was trained using only manufacturable designs. A scripting approach was used to generate the synthetic training dataset that was represented as voxel models. In their approach, however, four voxel models were required per part since four voxel scales were used for training (4, 8, 16, and 32 voxels per coordinate direction). Another consequence of the approach was that a volume fraction constraint could not be specified. Due to the training set size, training took considerable time (over 3 weeks with 20,000 part models). Additionally, they could not modify existing designs to improve their manufacturability.

A different approach was taken by Mohseni and Khodaygan [98]. They used a combination of techniques to apply DFM rules to AM parts, including a convolutional residual autoencoder for rounding and filleting sharp corners, transfer learning for reshaping circular holes into diamond shapes and increasing thickness of thin walls, a GAN for generating training datasets, and ResNet-18 for classification of build orientations to reduce support structures.

Several recent works proposed ML methods for generating lattice and triply periodic minimal surface (TPMS) unit cells. For example, Jadhav et al. [99] developed a 3D diffusion model to generate a variety of architected metamaterial unit cells for target stiffness properties. Figure 6 shows the workflow of their approach. Their equation generator generates equations of single and hybrid TPMS structures where sigmoid and various trigonometric equations are used to combine two or three TPMS structures. They utilized an implicit representation to perform reasoning. The training process covers steps a–g, while steps h–j represent the inference where new TPMS structures are generated. From their implicit representation, they can generate voxel models for structural analysis (steps b and c) and mesh models for visualization and fabrication (step j).

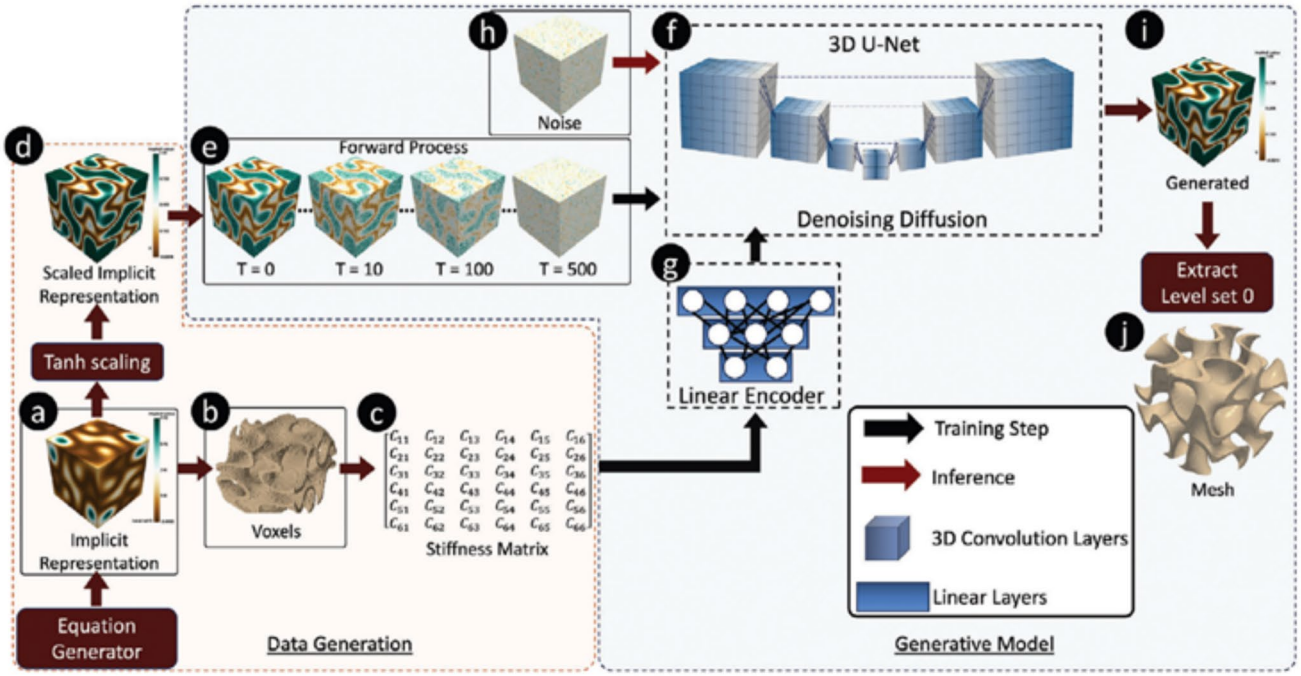

Fig. 6 Workflow of the cellular structure unit cell generation system. Steps a–g represent the training workflow, while steps h–j represent inference where a new structure is generated [99]

5.2 NN-based co-optimization

A neural network-based computational framework was developed for the simultaneous optimization of the shape, layers, and fiber paths of fiber-reinforced composites [100]. Both anisotropic strength and manufacturability were optimization objectives. The framework employs three neural networks that model implicit neural fields to represent the part shape, layer sequence, and fiber orientation. A solid isotropic material penalization (SIMP)-based topology optimization framework was adapted for this co-optimization problem. More specifically, the three neural fields include a density field for material distribution, a field for the order of material deposition, indicating layers, and a fiber orientation field. The authors show that their approach enables an integrated, differentiable process that optimizes both structural performance and the manufacturing process, in this case, FFF of both polymer and reinforcing fibers. With differentiable objective and constraint functions, gradient-based optimization algorithms can be used to solve the co-optimization problem, which is important from a computational efficiency perspective. Physical experiments demonstrated the effectiveness of the method.

5.3 DFM via image modification

To overcome the limitations of other ML approaches to DFM, a new approach was proposed that identified manufacturing features in the part, then modified their shape according to manufacturability rules for a given process.

Wang et al. proposed the Manufacturable conditional GAN (McGAN) as an implementation of that approach for parts to be injection molded [101]. The framework for McGAN is shown in Fig. 7. Given a 2D part representation (image), instance segmentation was performed using Mask R-CNN to segment the part into multiple simple features [102]. Each manufacturability rule was embodied in a conditional GAN, based on the Pix2Pix GAN [103], that modified a feature shape based on the rule. As a result, each shape should now be manufacturable [103]. After shape modifications, the part features are assembled into a complete part representation (modified image) as shown on the right side of Fig. 7. In this work, three manufacturability rules were implemented using Pix2Pix: rounding sharp corners, adding draft angles, and reducing feature height/width aspect ratios according to typical molding limitations. The results of McGAN were promising as modified designs were of high quality from the viewpoint of manufacturability [101].

Although McGAN worked well at modifying 2D part representations for molding considerations, the approach is insufficient for DFM for two primary reasons. First, of course, DFM needs to be applied in 3D. Second, modified designs must also meet functional requirements. In preliminary work, McGAN was extended to 3D and integrated with a VAE that implemented shape optimization in a manner analogous to the TO approach from Wang et al. [89]. Mask

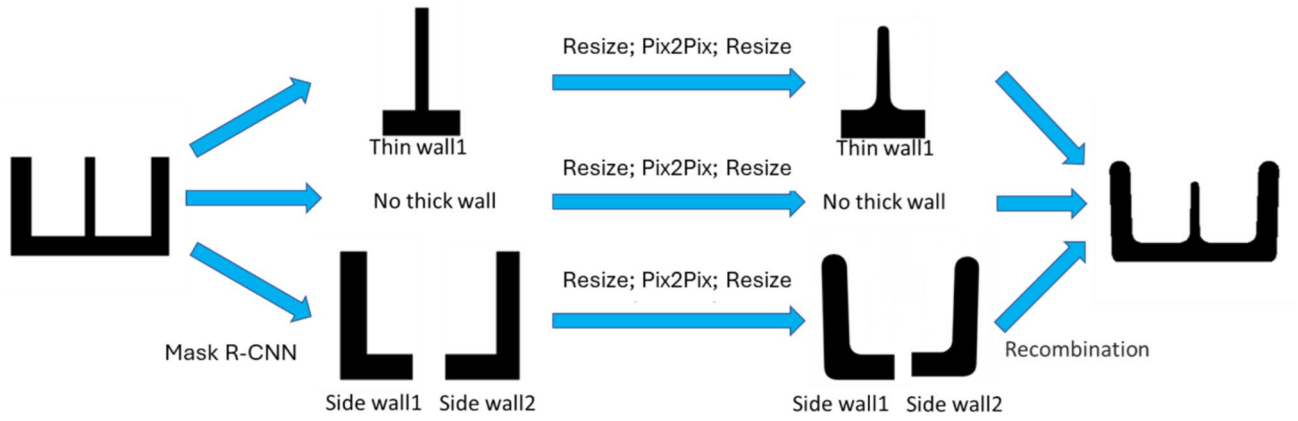

Fig. 7 The framework of McGAN for injection molding as presented in [101]

R-CNN was extended to segment 3D voxel models, instead of 2D images, and Pix2Pix was extended to 3D Vox2Vox to implement the three manufacturability rules of rounding corners, adding draft, and reducing aspect ratios.

For functional design, the VAE architecture utilized the typical encoder-decoder approach, with five 3D convolution layers, resulting in a $1 \times 1 \times 256$ output vector that represented 128 mean values and 128 standard deviations, while the decoder had 6 transpose convolution layers. The VAE was trained on 10,000 rectangular parts representing product housings with various internal features.

Manual iterations were used to integrate the functional design VAE with the McGAN DFM capability. In experiments, only 2–3 iterations were necessary between functional design and DFM. After each design generation step with the VAE, the designs were evaluated using 3D structural FEA to determine their compliance (optimization objective) and volume fraction. After evaluating all designs, the Pareto front was identified, and the top set of designs was selected for subsequent DFM. Each selected design was then modified using the 3D version of McGAN. This set of modified designs was then sent back to the VAE which generated a new batch of designs. This VAE-DFM iteration continued until the DFM module made minimal changes to the designs from the VAE (minimal was approximately 2% of voxels changed).

The design problem that illustrates the use of the VAE-DFM system is shown in Fig. 8. This is a rectangular product housing component with two internal ribs and a hole surrounded by an internal wall. The objective is to maximize stiffness under a distributed load on the bottom surface, with a fixed boundary condition around the open perimeter. A volume fraction constraint was specified as well. The part design domain was discretized into

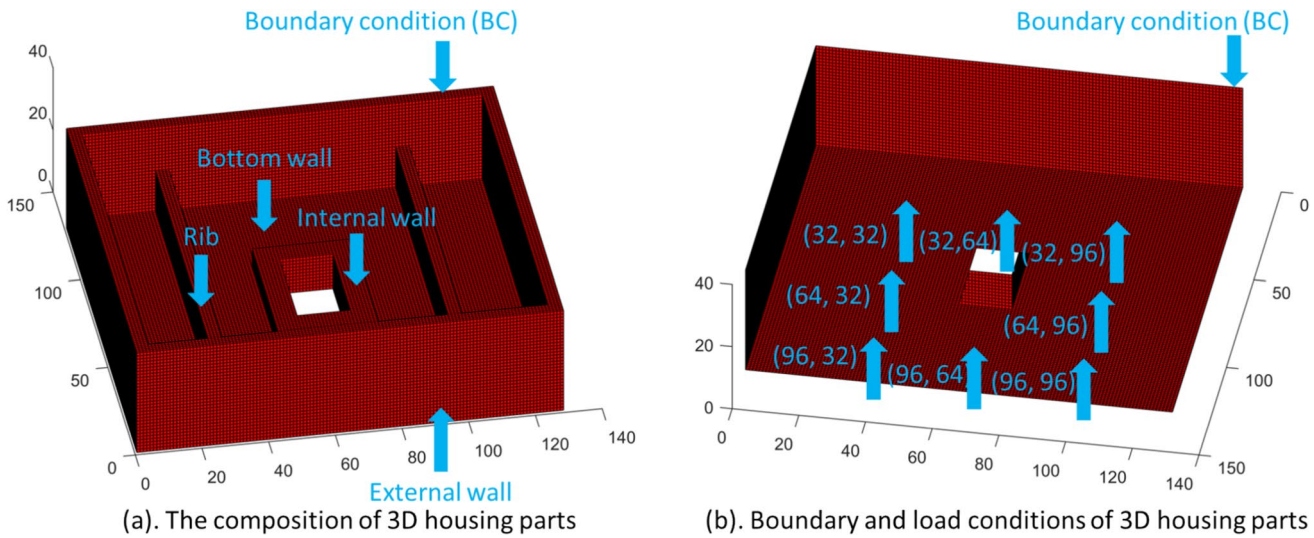

Fig. 8 The 3D housing part design problem: **a** composition and **b** load and boundary conditions [104]

a $128 \times 128 \times 32$ voxel space that resulted in a total of 107,000,000 possible designs [104].

Four generated part designs are shown in Fig. 9, one design per row. The left column represents inputs to the DFM cGAN, while the middle and right columns show top and bottom views of the resulting part designs. As expected, all part designs have rounded corners and draft angles on the vertical walls and rib features. Aspect ratio limits were achieved for the internal features as well. Note the slots that were added to the undersides of the thick rib features in Designs 1 and 4 (visible in the right column). Such slots are often added under thick features to achieve uniform wall thickness throughout a part, and examples were included in the 3D McGAN training dataset.

McGAN works well on a wide range of part designs consisting of 3 or 5 vertical walls in 2D and rectangular housings with internal features in 3D, but it has some limitations. The image modification approach is performed on a feature-by-feature basis after segmentation. The Mask R-CNN GAN needs to be trained to recognize each feature type of interest; however, if a shape feature or feature combination is not recognized, segmentation will likely fail. Currently, the only feature interactions considered are vertical-to-horizontal wall interactions. Then, Pix2Pix or Vox2Vox GANs, trained for each type of feature, are applied to modify the feature

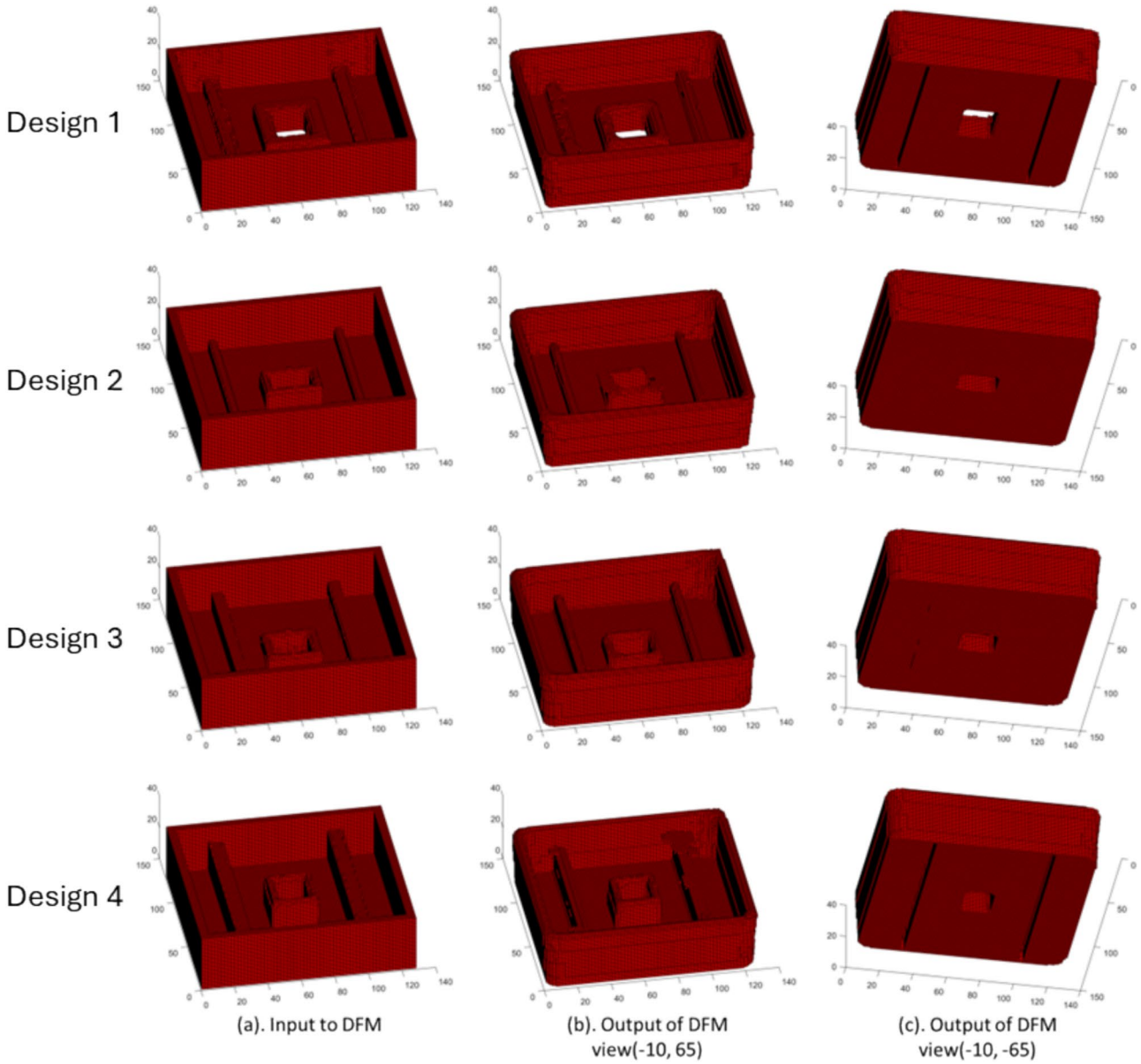

Fig. 9 Four designs produced in the iterative functional design and DFM process for the design problem shown in Fig. 8 [104]

shape. Significant efforts are needed to generate training datasets for both segmentation and modification. Generality and scalability to additional design rules and manufacturing processes remain limited, and further research is needed.

More generally, the issue of which part representation to use for design modifications requires future investigation. Take the problem of learning how to modify part geometry to change the draft angle. A user of a CAD system can add draft to a part model with one command. Behind the scenes, the CAD system changes the orientation of each vertical surface by the specified draft angle; that is, one parameter is changed for each affected surface, which, for most parts, is on the order of tens of operations. In contrast, changing the draft angle for a 2D image or a 3D voxel model can involve moving hundreds or thousands of elements. It may be much easier to train ML models to operate on BRep models, where surfaces are modeled explicitly, than to operate on image and voxel models. Graph-based neural networks that operate on face-adjacency graphs, or other BRep-based representations, may become easier to train and more generalizable than the well-known image-based network technologies for design applications.

6 Conclusions

AI and ML technologies have matured to the point where they are impacting the AM field significantly. This paper provides a targeted review of AI/ML applications in AM, specifically in defect detection, surrogate modeling of AM processes, generative design, and design for manufacturing. Specific examples in each area are provided, along with broad introductions, instead of providing a fine-grained, comprehensive survey.

In the defect detection area, a wide range of sensors is available in commercial PFB and DED machines that provide rich data streams for ML models to analyze. Excellent results have been achieved for porosity, lack of fusion, and crack prediction, poor bonding identification, and warpage, distortion, and other dimensional accuracy estimation. Early applications used conventional ML techniques and CNNs to analyze images to identify likely defects. More recently, more sophisticated techniques have been tested, including LSTM methods for analyzing time-series data streams, transformer-based models for multi-sensor fusion, and diffusion probabilistic models, particularly when datasets are limited. Challenges, limitations, and promising research directions were identified; they were related to difficulties in detecting multiple defect types, ML model generalizability, and training data scarcity and imbalance.

Surrogate models have demonstrated very good capabilities in predicting residual stresses and warpage in PBF-fabricated parts, replacing high fidelity and computationally expensive process simulations. 3D CNNs successfully learned from simulations of training models to predict the results of unseen test models. Increasingly, physics-informed neural networks (PINN) are being applied to embed some of the physics of powder melting, heat transfer, and solidification into the NN. Additionally, a method for processing time-series data, the bi-directional LSTM, demonstrated excellent performance in predicting residual stresses. The LSTM-based approach was explored because the layer-by-layer nature of AM fabrication could be interpreted as time-series data. The model was compared with the results from a 3D CNN model and showed better performance. Additional investigations into emerging AI techniques and combinations of AI techniques are likely to yield even better prediction results in the future. Challenges and research directions were similar to those in the defect detection area: narrowness of model applicability, lack of generalizability, and the expense of training dataset development.

Generative design has been available commercially for over a decade as an ML-augmented TO technology for structural design generation at first, and has been extended to thermal, fluid, and other physical principle-based design problems. In the research realm, a variety of approaches have been investigated, combining ML and TO methods, including ML and TO iteratively improving on design results, ML embedded in TO, and TO embedded in ML. With the rapid maturation of large language models and foundation models, the possibilities for generative design are enormous. However, it is necessary for the AI-generated models to be grounded in correct physics and to be based on the rich and varied information models used in engineering. These advances will require significant effort.

Design for additive manufacturing is relatively less explored compared to other topics covered in this paper. Some examples include DFM for conventional manufacturing processes, but these approaches have potential applications to AM. Several very different approaches were presented. The first embedded a GAN model into the TO formulation to optimize manufacturable designs for the 3-axis machining process, while the second proposed a co-optimization framework that used neural networks to model scalar fields, representing structural and manufacturing design spaces. The third demonstrated how DFM rules can be embodied as cGANs and how molded parts can be modified according to those rules. AI-based DFM and DFAM remain nascent. From the literature, research directions remain uncertain. However, the potential for combining generative design and DFM seems very promising.

Acknowledgements The authors gratefully acknowledge funding from the US National Science Foundation Future Manufacturing Research Grant #2229260. DWR gratefully acknowledges funding from the Singapore RIE2025 Manufacturing, Trade and Connectivity (MTC) Programmatic Fund, Grant No: M24N3b0028.

Author contribution David Rosen: writing—original draft, review, editing, conceptualization, methodology, supervision, funding acquisition. Xiaofang Liu: writing—original, review and editing.

Funding The authors gratefully acknowledge funding from the US National Science Foundation Future Manufacturing Research Grant #2229260. DWR gratefully acknowledges funding from the Singapore RIE2025 Manufacturing, Trade and Connectivity (MTC) Programmatic Fund, Grant No: M24N3b0028.

Data availability The authors did not collect data as part of this research. Therefore, there are no data available.

Declarations

Competing interests The authors have no competing interests that are relevant to the content of this article. The authors have no financial or proprietary interests in any material discussed in this article.

References

1. Gibson I, Rosen D, Stucker B, Khorasani M (2021) Additive manufacturing technologies, Third ed. Springer. https://doi.org/10.1007/978-3-030-56127-7
2. Qin J, Hu F, Liu Y, Witherell P, Wang CCL, Rosen DW et al (2022) Research and application of machine learning for additive manufacturing. Addit Manuf. https://doi.org/10.1016/j.addma.2022.102691
3. Xames MD, Torsha FK, Sarwar F (2023) A systematic literature review on recent trends of machine learning applications in additive manufacturing. J Intell Manuf 34(6):2529–2555. https://doi.org/10.1007/s10845-022-01957-6
4. Herzog T, Brandt M, Trinchi A, Sola A, Molotnikov A (2024) Process monitoring and machine learning for defect detection in laser-based metal additive manufacturing. J Intell Manuf 35(4):1407–37. https://doi.org/10.1007/s10845-023-02119-y
5. Ng WL, Goh GL, Goh GD, Ten JSJ, Yeong WY (2024) Progress and opportunities for machine learning in materials and processes of additive manufacturing. Adv Mater. https://doi.org/10.1002/adma.202310006
6. Ukwaththa J, Herath S, Meddage DPP (2024) A review of machine learning (ML) and explainable artificial intelligence (XAI) methods in additive manufacturing (3D printing). Mater Today Commun. https://doi.org/10.1016/j.mtcomm.2024.110294
7. Jin LC, Zhai XY, Wang K, Zhang K, Wu DZ, Nazir A et al (2024) Big data, machine learning, and digital twin assisted additive manufacturing: a review. Materials & Design. https://doi.org/10.1016/j.matdes.2024.113086
8. Chua ZY, Ahn IH, Moon SK (2017) Process monitoring and inspection systems in metal additive manufacturing: status and applications. Int J Pr Eng Man-Gt 4(2):235–245. https://doi.org/10.1007/s40684-017-0029-7
9. Stajkovic J, Kahl M, Kaserer L, Braun J, Scheuringer S, Mayr-Schmölzer B et al (2025) Correlating dimensionless enthalpy, pyrometry, and melt pool geometry within the laser powder bed fusion energetic regime: a path to in-situ melt pool control demonstrated on tungsten. J Manuf Process 141:1310–23. https://doi.org/10.1016/j.jmapro.2025.03.033
10. Pfaff A, Schäffer S, Jäcklein M, Balle F (2023) Measuring the cooling behavior of melt pools in L-PBF by pyrometry. Materials. https://doi.org/10.3390/ma16103647
11. Vallabh CKP, Zhao XY (2022) Melt pool temperature measurement and monitoring during laser powder bed fusion based additive manufacturing via single-camera two-wavelength imaging pyrometry (STWIP). J Manuf Process 79:486–500. https://doi.org/10.1016/j.jmapro.2022.04.058
12. Li X, Li H, Shen S, Chen L, Liu S, Dai L et al (2025) In-situ coaxial temperature monitoring of LPBF melt pool by a compact dual-wavelength thermometry system (CDWTS). Opt Lasers Eng 194:109194. https://doi.org/10.1016/j.optlaseng.2025.109194
13. Ikeshoji TT, Yonehara M, Kato C, Yanaga Y, Takeshita K, Kyogoku H (2022) Spattering mechanism of laser powder bed fusion additive manufacturing on heterogeneous surfaces. Sci Rep. https://doi.org/10.1038/s41598-022-24828-9
14. Bitharas I, Parab N, Zhao C, Sun T, Rollett AD, Moore AJ (2022) The interplay between vapour, liquid, and solid phases in laser powder bed fusion. Nat Commun. https://doi.org/10.1038/s41467-022-30667-z
15. Guerra MG, Errico V, Fusco A, Lavecchia F, Campanelli SL, Galantucci LM (2022) High resolution-optical tomography for in-process layerwise monitoring of a laser-powder bed fusion technology. Addit Manuf. https://doi.org/10.1016/j.addma.2022.102850
16. Sen C, Sail G, Subasi L, Oren S, Dursun G, Orhangul A (2024) In-situ surface roughness evaluation of laser powder bed fusion surfaces using optical tomography. Procedia CIRP 123:363–368. https://doi.org/10.1016/j.procir.2024.05.064
17. Guerra MG, Lafirenza M, Errico V, Angelastro A (2023) In-process dimensional and geometrical characterization of laser-powder bed fusion lattice structures through high-resolution optical tomography. Opt Laser Technol. https://doi.org/10.1016/j.optlastec.2023.109252
18. O'Dowd NM, Wachtor AJ, Todd MD (2021) Effects of digital fringe projection operational parameters on detecting powder bed defects in additive manufacturing. Addit Manuf. https://doi.org/10.1016/j.addma.2021.102454
19. Zhang YZ, Zhang P, Jiang X, Zhang SY, Zhong K, Li ZW (2023) In-situ 3d contour measurement for laser powder bed fusion based on phase guidance. Theor Appl Mech Lett. https://doi.org/10.1016/j.taml.2022.100405
20. Remani A, Rossi A, Peña F, Thompson A, Dardis J, Jones N et al (2024) In-situ monitoring of laser-based powder bed fusion using fringe projection. Addit Manuf. https://doi.org/10.1016/j.addma.2024.104334
21. Song JY, Dass A, Moridi A, McLaskey GC (2024) Detection of defects during laser-powder interaction by acoustic emission sensors and signal characteristics. Addit Manuf. https://doi.org/10.1016/j.addma.2024.104035
22. Herzog T, Brandt M, Trinchi A, Sola A, Hagenlocher C, Molotnikov A (2024) Defect detection by multi-axis infrared process monitoring of laser beam directed energy deposition. Sci Rep. https://doi.org/10.1038/s41598-024-53931-2
23. Aggarwal A, Pandiyan V, Leinenbach C, Leparoux M (2024) Investigating laser beam shadowing and powder particle dynamics in directed energy deposition through high-fidelity modelling

and high-speed imaging. Addit Manuf. https://doi.org/10.1016/j.addma.2024.104344
24. Ansari MJ, Roccisano A, Arcondoulis EJG, Schulz C, Schläfer T, Hall C (2025) Relationship between associated acoustic emission and crack position during directed energy deposition of a metal matrix composite. J Manuf Process 147:177–190. https://doi.org/10.1016/j.jmapro.2025.05.015
25. Ansari MJ, Arcondoulis EJG, Roccisano A, Schulz C, Schlaefer T, Hall C (2024) Optimized analytical approach for the detection of process-induced defects using acoustic emission during directed energy deposition process. Addit Manuf. https://doi.org/10.1016/j.addma.2024.104218
26. Wang RX, Garcia D, Kamath RR, Dou CR, Ma XH, Shen B et al (2022) In situ melt pool measurements for laser powder bed fusion using multi sensing and correlation analysis. Sci Rep. https://doi.org/10.1038/s41598-022-18096-w
27. Zalameda JN, Hocker SJ, Spaeth PW, Widener B, editors. In situ inspection of laser powder bed fusion Ti-6AL-4V additive manufacturing using an infrared sensor. Thermosense: Thermal Infrared Applications XLVII; 2025: SPIE. https://doi.org/10.1117/12.3054069.
28. Gaikwad A, Williams RJ, de Winton H, Bevans BD, Smoqi Z, Rao PHLD, et al. Multi phenomena melt pool sensor data fusion for enhanced process monitoring of laser powder bed fusion additive manufacturing. Mater Design 2022;221. https://doi.org/10.1016/j.matdes.2022.110919.
29. Ansari MA, Crampton A, Garrard R, Cai BA, Attallah M (2022) A convolutional neural network (CNN) classification to identify the presence of pores in powder bed fusion images. Int J Adv Manuf Technol 120(7–8):5133–5150. https://doi.org/10.1007/s00170-022-08995-7
30. Wu QR, Yang F, Lv CM, Liu CM, Tang WL, Yang JQ (2024) In-situ quality intelligent classification of additively manufactured parts using a multi-sensor fusion based melt pool monitoring system. Addit Manuf Front 3(3):200153. https://doi.org/10.1016/j.amf.2024.200153
31. Shi S, Liu XW, Wang ZG, Chang H, Wu YN, Yang R et al (2024) An intelligent process parameters optimization approach for directed energy deposition of nickel-based alloys using deep reinforcement learning. J Manuf Process 120:1130–40. https://doi.org/10.1016/j.jmapro.2024.05.001
32. Schürmann M, Varshneya S, Klar M, Ghansiyal S, Kloft M, Aurich JC (2025) A framework for in-situ process control in metal additive manufacturing using anomaly-driven reinforcement learning. Procedia CIRP 134:211–216. https://doi.org/10.1016/j.procir.2025.03.050
33. Cannizzaro D, Antonioni P, Ponzio F, Galati M, Patti E, Di Cataldo S (2025) Machine learning-enabled real-time anomaly detection for electron beam powder bed fusion additive manufacturing. J Intell Manuf 36(3):2105–2119. https://doi.org/10.1007/s10845-024-02359-6
34. Pandiyan V, Masinelli G, Claire N, Tri LQ, Hamidi-Nasab M, de Formanoir C, et al. Deep learning-based monitoring of laser powder bed fusion process on variable time-scales using heterogeneous sensing and X-ray radiography guidance. Addit Manuf 2022;58. https://doi.org/10.1016/j.addma.2022.103007.
35. Chen LQ, Yao XL, Tan CL, He WY, Su JL, Weng F et al (2023) In-situ crack and keyhole pore detection in laser directed energy deposition through acoustic signal and deep learning. Addit Manuf. https://doi.org/10.1016/j.addma.2023.103547
36. Surovi NA, Hussain S, Soh GS. A study of machine learning framework for enabling early defect detection in wire arc additive manufacturing processes. Proceedings of Asme 2022 International Design Engineering Technical Conferences and Computers and Information in Engineering Conference, Idetc-Cie2022, Vol 3a 2022. https://doi.org/10.1115/DETC2022-89164.
37. Zhang H, Wu QR, Tang WL, Yang JQ (2024) Acoustic signal-based defect identification for directed energy deposition-arc using wavelet time-frequency diagrams. Sensors. https://doi.org/10.3390/s24134397
38. Petrich J, Snow Z, Corbin D, Reutzel EW (2021) Multi-modal sensor fusion with machine learning for data-driven process monitoring for additive manufacturing. Addit Manuf. https://doi.org/10.1016/j.addma.2021.102364
39. Chen LQ, Moon SK (2024) In-situ defect detection in laser-directed energy deposition with machine learning and multi-sensor fusion. J Mech Sci Technol 38(9):4477–4484. https://doi.org/10.1007/s12206-024-2401-1
40. Papatheodorou A, Papadimitriou N, Stathatos E, Benardos P, Vosniakos G-C (2025) Recent advances in sensor fusion monitoring and control strategies in laser powder bed fusion: a review. Machines. https://doi.org/10.3390/machines13090820
41. Pandiyan V, Drissi-Daoudi R, Shevchik S, Masinelli G, Tri LQ, Logé R, et al. Deep transfer learning of additive manufacturing mechanisms across materials in metal-based laser powder bed fusion process. J Mater Process Tech 2022;303. https://doi.org/10.1016/j.jmatprotec.2022.117531.
42. Farea SM, Unel M, Koc B, editors. Defect prediction in directed energy deposition using an ensemble of clustering models. 2024 IEEE 22nd International Conference on Industrial Informatics (INDIN); 2024 18–20 Aug. 2024. https://ieeexplore.ieee.org/document/10774281.
43. Zhu QM, Liu ZL, Yan JH (2021) Machine learning for metal additive manufacturing: predicting temperature and melt pool fluid dynamics using physics-informed neural networks. Comput Mech 67(2):619–635. https://doi.org/10.1007/s00466-020-01952-9
44. Han R, Wang YZ, Guo WH, Wang CW, Zhang YH, Zi YY et al (2025) DDEG: addressing data scarcity in additive manufacturing defect detection through joint generation of CT images and defect annotations. Adv Eng Inform. https://doi.org/10.1016/j.aei.2025.103619
45. Ogoke F, Suresh SK, Adamczyk J, Bolintineanu D, Garland A, Heiden M et al (2025) Deep learning based optical image super-resolution via generative diffusion models for layerwise in-situ LPBF monitoring. Addit Manuf 107:104790. https://doi.org/10.1016/j.addma.2025.104790
46. Safdar M, Wood G, Zimmermann M, Lamouche G, Wanjara P, Zhao YF. Detecting the extent of co-existing anomalies in additively manufactured metal matrix composites through explainable selection and fusion of multi-camera deep learning features. Virtual Phys Prototy 2025;20(1). https://doi.org/10.1080/17452759.2025.2515240.
47. Farbiz F, Balaraman RK, Tan QY, Jarary-Zadeh M, Ford CS, Kgee JO, et al. AI-enabled processing of online sensor data for defect detection in metal additive manufacturing. submitted, Journal of Intelligent Manufacturing 2024.
48. Kouraytem N, Li XX, Tan WD, Kappes B, Spear AD (2021) Modeling process-structure-property relationships in metal additive manufacturing: a review on physics-driven versus data-driven approaches. J Phys-Mater. https://doi.org/10.1088/2515-7639/abca7b
49. Nath P, Hu Z, Mahadevan S, editors. Modeling and uncertainty quantification of material properties in additive manufacturing. AIAA SciTech Forum, 2018 (2018–0923); 2018 7 Jan https://doi.org/10.2514/6.2018-0923.
50. Tapia G, Khairallah S, Matthews M, King WE, Elwany A (2018) Gaussian process-based surrogate modeling framework for process planning in laser powder-bed fusion additive manufacturing of 316L stainless steel. Int J Adv Manuf Technol 94(9–12):3591–603. https://doi.org/10.1007/s00170-017-1045-z

51. Kumar HA, Kumaraguru S, Paul CP, Bindra KS (2021) Faster temperature prediction in the powder bed fusion process through the development of a surrogate model. Opt Laser Technol. https://doi.org/10.1016/j.optlastec.2021.107122
52. Li JR, Jin R, Yu HZ (2018) Integration of physically-based and data-driven approaches for thermal field prediction in additive manufacturing. Mater Des 139:473–485. https://doi.org/10.1016/j.matdes.2017.11.028
53. Roy M, Wodo O (2020) Data-driven modeling of thermal history in additive manufacturing. Addit Manuf. https://doi.org/10.1016/j.addma.2019.101017
54. Thinh T-Q-D, Hoang V, Tran XV, Fetni S, Duchêne L, Tran H, et al. Characterization, propagation, and sensitivity analysis of uncertainties in the directed energy deposition process using a deep learning-based surrogate model. Probabilistic Engineering Mechanics 2022;69:103297. https://doi.org/10.1016/j.probengmech.2022.103297.
55. Hemmasian A, Ogoke F, Akbari P, Malen J, Beuth J, Barati Farimani A (2023) Surrogate modeling of melt pool temperature field using deep learning. Addit Manuf Lett 5:100123. https://doi.org/10.1016/j.addlet.2023.100123
56. Wu SH, Tariq U, Joy R, Mahmood MA, Malik AW, Liou F (2024) A robust recurrent neural networks-based surrogate model for thermal history and melt pool characteristics in directed energy deposition. Materials. https://doi.org/10.3390/ma17174363
57. Lestandi L, Wong J, Dong GY, Kuehsamy SJ, Mikula J, Vastola G et al (2024) Data-driven surrogate modelling of residual stresses in laser powder-bed fusion. Int J Comput Integr Manuf 37(6):685–707. https://doi.org/10.1080/0951192X.2023.2257628
58. Hosseini E, Scheel P, Müller O, Molinaro R, Mishra S (2023) Single-track thermal analysis of laser powder bed fusion process: parametric solution through physics-informed neural networks. Comput Methods Appl Mech Eng. https://doi.org/10.1016/j.cma.2023.116019
59. Safari H, Wessels H. Physics-informed surrogates for temperature prediction of multi-tracks in laser powder bed fusion. 2025. https://doi.org/10.48550/arXiv.2502.01820.
60. Chung Baek A, Kim T, Seong M, Lee S, Kang H, Park E et al (2025) Multimodal deep learning for enhanced temperature prediction with uncertainty quantification in directed energy deposition (DED) process. Virtual Phys Prototyp. https://doi.org/10.1080/17452759.2025.2474532
61. Kannapinn M, Roth F, Weeger O. Digital twin inference from multi-physical simulation data of DED additive manufacturing processes with neural ODEs. arXiv preprint arXiv:241203295 2024. https://doi.org/10.48550/arXiv.2412.03295.
62. Peng B, Panesar A (2025) Multi-layer thermal history prediction framework for directed energy deposition based on extended physics-informed neural networks (XPINN). Addit Manuf 110:104953. https://doi.org/10.1016/j.addma.2025.104953
63. Srinivasan S, Swick B, Groeber MA (2020) Laser powder bed fusion parameter selection via machine-learning-augmented process modeling. JOM 72(12):4393–403. https://doi.org/10.1007/s11837-020-04383-2
64. Ren Y, Wang Q (2022) Gaussian-process based modeling and optimal control of melt-pool geometry in laser powder bed fusion. J Intell Manuf 33(8):2239–2256. https://doi.org/10.1007/s10845-021-01781-4
65. Cao YH, Chen CY, Xu SZ, Zhao RX, Guo K, Hu T et al (2024) Machine learning assisted prediction and optimization of mechanical properties for laser powder bed fusion of Ti6Al4V alloy. Addit Manuf. https://doi.org/10.1016/j.addma.2024.104341
66. Butt MM, Rashid S, Haq MU, Mustafa A, Iqbal A, Laieghi H et al (2025) Machine learning driven prediction and GUI based optimization of quasi-static mechanical properties in SLM fabricated Ti6Al4V alloy. Int J Precis Eng Manuf. https://doi.org/10.1007/s12541-025-01360-0
67. Qin J, Liu Y, Grosvenor R, Lacan F, Jiang ZG (2020) Deep learning-driven particle swarm optimisation for additive manufacturing energy optimisation. J Clean Prod. https://doi.org/10.1016/j.jclepro.2019.118702
68. Costa A, Buffa G, Palmeri D, Pollara G, Fratini L (2022) Hybrid prediction-optimization approaches for maximizing parts density in SLM of Ti6Al4V titanium alloy. J Intell Manuf 33(7):1967–1989. https://doi.org/10.1007/s10845-022-01938-9
69. Dong GY, Lestandi L, Mikula J, Vastola G, Kizhakkinan U, Wang JC, et al. A part-scale, feature-based surrogate model for residual stresses in the laser powder bed fusion process. J Mater Process Tech 2022;304. https://doi.org/10.1016/j.jmatprotec.2022.117541.
70. Vulimiri PS, Riley S, Dugast FX, To AC (2025) A mean-variance estimation bidirectional convolutional long short-term memory surrogate model predicting residual stress and model error for laser powder bed fusion. Addit Manuf. https://doi.org/10.1016/j.addma.2024.104591
71. Mikula J, Ahluwalia R, Laskowski R, Wang K, Vastola G, Zhang YW (2021) Modelling the influence of process parameters on precipitate formation in powder-bed fusion additive manufacturing of IN718. Mater Des. https://doi.org/10.1016/j.matdes.2021.109851
72. Liu J, Ye JF, Izquierdo DS, Vinel A, Shamsaei N, Shao S (2023) A review of machine learning techniques for process and performance optimization in laser beam powder bed fusion additive manufacturing. J Intell Manuf 34(8):3249–3275. https://doi.org/10.1007/s10845-022-02012-0
73. Shin S, Shin D, Kang NM (2023) Topology optimization via machine learning and deep learning: a review. J Comput Des Eng 10(4):1736–1766. https://doi.org/10.1093/jcde/qwad072
74. Abueidda DW, Koric S, Sobh NA (2020) Topology optimization of 2D structures with nonlinearities using deep learning. Comput Struct. https://doi.org/10.1016/j.compstruc.2020.106283
75. Sharpe C, Seepersad CC, editors. Topology design with conditional generative adversarial Networks2019. Volume 2A: 45th Design Automation ConferenceASME 2019 International Design Engineering Technical Conferences and Computers and Information in Engineering Conference. https://doi.org/10.1115/DETC2019-97833.
76. Rawat S, Shen M-HH (2018) A novel topology design approach using an integrated deep learning network architecture. ArXiv. https://doi.org/10.48550/arXiv.1808.02334
77. Rawat S, Shen M-HH. Application of adversarial networks for 3D Structural topology optimization. SAE Technical Paper 2019–01–0829 2019. https://doi.org/10.4271/2019-01-0829.
78. Rawat S, Shen M-HH (2019) A novel topology optimization approach using conditional deep learning. ArXiv. https://doi.org/10.48550/arXiv.1901.04859
79. Zheng S, He ZZ, Liu HL (2021) Generating three-dimensional structural topologies via a U-Net convolutional neural network. Thin-Walled Struct. https://doi.org/10.1016/j.tws.2020.107263
80. Zhang Y, Chen A, Peng B, Zhou X, Wang D (2019) A deep convolutional neural network for topology optimization with strong generalization ability. ArXiv. https://doi.org/10.48550/arXiv.1901.07761
81. Nie ZG, Lin T, Jiang HL, Kara LB (2021) Topologygan: topology optimization using generative adversarial networks based on physical fields over the initial domain. J Mech Des. https://doi.org/10.1115/1.4049533

82. Deng CY, Wang YZ, Qin C, Fu Y, Lu W (2022) Self-directed online machine learning for topology optimization. Nat Commun. https://doi.org/10.1038/s41467-021-27713-7
83. Chen HR, Joglekar A, Kara LB. Topology optimization using neural networks with conditioning field initialization for improved efficiency. J Mech Design 2024;146(6). https://doi.org/10.1115/1.4064131.
84. Seo J, Kapania RK (2023) Topology optimization with advanced CNN using mapped physics-based data. Struct Multidiscip Optim. https://doi.org/10.1007/s00158-022-03461-0
85. Yan J, Zhou MF, Xu Q, Du HZ (2025) Deep learning-driven topology optimization using principal stress information based on assumed source point. Eng Struct. https://doi.org/10.1016/j.engstruct.2025.121203
86. Yu Y, Hur T, Jung J, Jang IG (2019) Deep learning for determining a near-optimal topological design without any iteration. Struct Multidiscip Optim 59(3):787–799. https://doi.org/10.1007/s00158-018-2101-5
87. Li BT, Huang CJ, Li X, Zheng S, Hong J (2019) Non-iterative structural topology optimization using deep learning. Comput Aided Des 115:172–180. https://doi.org/10.1016/j.cad.2019.05.038
88. Oh S, Jung Y, Kim S, Lee I, Kang N (2019) Deep generative design: integration of topology optimization and generative models. J Mech Des. https://doi.org/10.1115/1.4044229
89. Wang ZC, Melkote S, Rosen DW (2023) Generative design by embedding topology optimization into conditional generative adversarial network. J Mech Des. https://doi.org/10.1115/1.4062980
90. Jang S, Yoo S, Kang N (2022) Generative design by reinforcement learning: enhancing the diversity of topology optimization designs. Comput-Aided Des. https://doi.org/10.1016/j.cad.2022.103225
91. Yamasaki S, Yaji K, Fujita K (2021) Data-driven topology design using a deep generative model. Struct Multidiscip Optim 64(3):1401–1420. https://doi.org/10.1007/s00158-021-02926-y
92. Shu D, Cunningham J, Stump G, Miller SW, Yukish MA, Simpson TW et al (2020) 3D design using generative adversarial networks and physics-based validation. J Mech Des. https://doi.org/10.1115/1.4045419
93. Mazé F, Ahmed F, editors. Diffusion models beat GANs on topology optimization. Thirty-Seventh AAAI Conference on Artificial Intelligence, Vol 37 No 8; 2023. https://doi.org/10.1609/aaai.v37i8.26093.
94. Chen HR, Joglekar A, Whitefoot KS, Kara LB. Concurrent build direction, part segmentation, and topology optimization for additive manufacturing using neural networks. J Mech Design 2023;145(9). https://doi.org/10.1115/1.4062663.
95. Kumar NK, Manasa CM, Kumar BKP, Bali M. Reinforcement learning-based topology optimization for generative designed lightweight structures. Methodsx 2025;15. https://doi.org/10.1016/j.mex.2025.103539.
96. Karnewar A, Wang O. MSG-GAN: multi-scale gradients for generative adversarial networks. 2020 IEEE/CVF Conference on Computer Vision and Pattern Recognition (CVPR 2020)2020. p. 7796–805. https://ieeexplore.ieee.org/document/9156324.
97. Greminger M, editor Generative adversarial networks with synthetic training data for enforcing manufacturing constraints on topology optimization. ASME 2020 International Design Engineering Technical Conferences and Computers and Information in Engineering Conference; 2020. V11AT11A005. https://doi.org/10.1115/DETC2020-22399.
98. Mohseni M, Khodaygan S (2024) Design for additive manufacturing of topology-optimized structures based on deep learning and transfer learning. Rapid Prototyping J 30(7):1411–1433. https://doi.org/10.1108/RPJ-02-2024-0102
99. Jadhav Y, Berthel J, Hu CS, Panat R, Beuth J, Farimani AB. Generative lattice units with 3D diffusion for inverse design: GLU3D. Adv Funct Mater 2024;34(41). https://doi.org/10.1002/adfm.202404165.
100. Liu T, Zhang TY, Chen YX, Wang WM, Jiang Y, Hunag Y, et al. Neural co-optimization of structural topology, manufacturable layers, and path orientations for fiber-reinforced composites. ACM Trans Graph 2025;44(4). https://doi.org/10.1145/3730922.
101. Wang Z, Yan X, Melkote S, Rosen D (2025) McGAN: generating manufacturable designs by embedding manufacturing rules into conditional generative adversarial network. Adv Eng Inform 64:103074. https://doi.org/10.1016/j.aei.2024.103074
102. He K, Gkioxari G, Dollár P, Girshick R, editors. Mask R-CNN. 2017 IEEE International Conference on Computer Vision (ICCV); 2017 22–29 Oct. 2017. https://ieeexplore.ieee.org/abstract/document/8237584.
103. Isola P, Zhu JY, Zhou T, Efros AA, editors. Image-to-image translation with conditional adversarial networks. 2017 IEEE Conference on Computer Vision and Pattern Recognition (CVPR); 2017 21–26 July 2017. https://ieeexplore.ieee.org/document/8100115.
104. Yan X, Wang Z, Melkote S, Rosen D. Machine learning-based cyber manufacturing services: a review of manufacturing process selection, process planning, and design for manufacturing. Engineering 2025.